VASCULAR SHUTDOWN AS AN EFFECT OF USING PHOTODYNAMIC THERAPY TO TREAT CANCER

by

Elizabeth Mary Pascucci

A thesis submitted in partial fulfillment
Of the requirements for the degree

of

Masters of Science

in

Microbiology

MONTANA STATE UNIVERSITY
Bozeman, Montana

December 2008

APPROVAL

of a thesis submitted by

Elizabeth Mary Pascucci

This thesis has been read by each member of the thesis committee and has been found to be satisfactory regarding content, English usage, format, citation, bibliographic style, and consistency, and is ready for submission to the Division of Graduate Education.

Dr. Jean Starkey

Approved for the Department of Microbiology

Dr. Mike Franklin

Approved for the Division of Graduate Education

Dr. Carl A. Fox

STATEMENT OF PERMISSION TO USE

In presenting this thesis in partial fulfillment of the requirements for a master's degree at Montana State University, I agree that the Library shall make it available to borrowers under rules of the Library.

If I have indicated my intention to copyright this thesis by including a copyright notice page, copying is allowable only for scholarly purposes, consistent with "fair use" as prescribed in the U.S. Copyright Law. Requests for permission for extended quotation from or reproduction of this thesis in whole or in parts may by granted only by the copyright beholder.

Elizabeth Mary Pascucci

December 2008

TABLE OF CONTENTS

TABLE OF CONTENTS – CONTINUED

LIST OF TABLES

Table Page

LIST OF FIGURES

LIST OF FIGURES - CONTINUED

Figure Page

ABSTRACT

Photodynamic therapy (PDT) is a treatment that uses the combination of a photosensitizing drug and light to selectively kill cancer cells. PDT has many potential advantages such as minimal side effects, excellent cosmetic results, and no cellular resistance burdening traditional cancer treatments such as chemotherapy and radiation. Currently used in the clinic, a limitation is depth of light penetration; therefore, PDT can only be used to treat superficial disease. Our novel PDT agent utilizes two-photon laser technology, which increases the depth of light penetration, greatly increasing the potential uses. Our PDT is able to kill selective cells because the PDT drug has a targeting agent so the drug only goes to cancer cells that overexpress the Somatostatin receptor 2 (SSTr2) on their cell surface. Laser light irradiates the cancer cells causing cytotoxic singlet oxygen to be produced damaging the cells. It was observed, through *in vivo* imaging of the tumors before and after treatment, that vascular flow was diminished as a result of PDT. It is well established that angiogenesis must occur when a tumor reaches a certain size in order for the cells to remain viable and the tumor to continue to grow; therefore, vascular shutdown could be an important mechanism of how PDT works. A series of experiments on the tumor vasculature using *in vivo* imaging, immunohistochemistry and confocal microscopy has taken place since this observation to determine what may be happening. Results of these studies have shown that tumor vessels do express the SSTr2 and therefore effected by treatment. Experiments using a somatostatin analog, octreoate, detected by a fluor has shown that the endothelial cells do take the drug up. To ensure that it is blood vessels that were being studied, tumor tissue was stained for both SSTr2 and vonWillebrand Factor (vWF), a recognized endothelial cell marker. Staining patterns for both antibodies were similar. To strengthen the argument, SSTr2- negative tumor cells also showed a positive staining pattern of their vessels, demonstrating that even though the tumor cells are SSTr2- negative, the tumor vessels can be SSTr2-positive and thus responsive to PDT.

CHAPTER 1

INTRODUCTION

Photodynamic Therapy

Photodynamic therapy (PDT) is an exciting approach to treating cancers and various other diseases. PDT involves the use of a photosensitizing drug and light to kill cells. A photosensitizer is a molecule that, when activated by light of the correct and specific wavelength in the presence of oxygen, can generate reactive oxygen species (9). PDT can be targeted to effect only cancer cells, producing death by necrosis and/or via the programmed cell death pathway, apoptosis. The protocol starts with an injected dose of the photosensitizing drug. If the drug is not designed to specifically target the tumor cells, it still can preferentially accumulate within tumor tissue versus normal tissue for a variety of reasons: elevated numbers of low-density lipoprotein receptors, presence of macrophages, decreased pH, abnormal stromal tissue, leaky vasculature, high levels of newly synthesized collagen, and high levels of lipids (2). Once the photosensitizing drug is taken up into the cells, a light source is used to illuminate the area. This light source is most often a laser. The drug, excited by absorption of the photons, undergoes one or more energy transitions emerging in the triplet state. The triplet may participate in one-electron oxidation/reduction reaction with a neighboring molecule which produces free radical intermediates that react with oxygen (2). This is known as a type I photochemical reaction. Alternatively or coincidentally, the more common type II photochemical

reaction can occur upon light absorption (Figure 1). In this reaction, the triplet-state photosensitizer can transfer energy to ground state oxygen, generating highly reactive and cytotoxic singlet oxygen (3). Due to the fact that singlet oxygen can migrate less than 0.02 μm after its formation, PDT only acts locally to effect cancer cells. Singlet oxygen exerts its irreversible cell damage by several methods: degrading lipids in cell membranes; increasing prostaglandin E2 levels; generating haematin aggregates; damaging the endothelial cells of blood vessels; inhibiting neoangiogenesis; and directly releasing cytochrome C from mitochondria (4). The photosensitizer can be regenerated for a subsequent activation. The success of PDT is multifactorial and depends on a number of factors including efficacy of preferential uptake and retention of the photosensitizer, correct wavelength and efficient absorption of light, (1) and presence of oxygen in type II reactions.

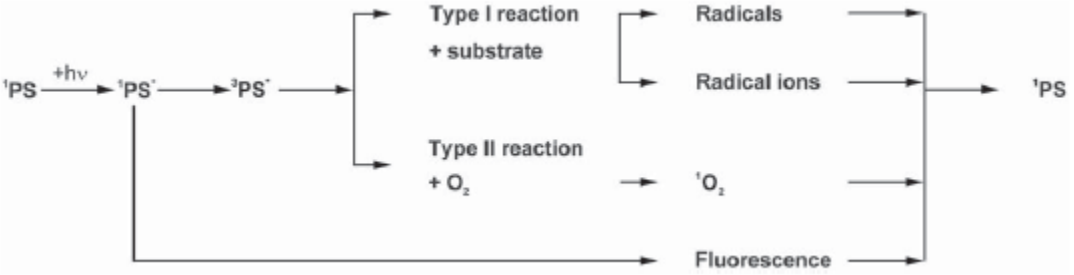

Figure 1. The principle of photodynamic therapy. This figure describes the energy transitions in the photosystem (PS) to ultimately create singlet oxygen ($^1O_2$). Figure used with permission from the author (5).

These reactions will only take place in cells where the photosensitizer has localized. Therefore, this type of therapy presents a favorable treatment option to current cancer treatments such as chemotherapy and radiation which damage cells throughout the entire body. PDT is comparatively non-invasive, it can be done as an outpatient

procedure, repeated doses can be given without the worry of generating cancer cell resistance, and the healing process results in little to no scarring (6).

Since the photosensitizing drug is such an important component of PDT, great care and consideration is taken in designing and synthesizing these drugs. It is important that the sensitizer be easy to administer systemically via injection. From this consideration water soluble sensitizers might be expected to be best since blood is water based (10). However, the sensitizer must also be able to enter cells, which involves traversing the lipid membrane, so the drugs also need to have some hydrophobic characteristics. Hydrophobic sensitizers are able to bind strongly to lipoproteins in the blood stream and be transported selectively to malignant tissue (10). Photosensitizers in use and under investigation are based on the tetrapyrrole nucleus; examples include porphyrin (hematoporphyrin derivative (HPD) or Photofrin® (Figure 2)), chlorins (benzoporphyrin derivative (BPD)), bacteriochlorins (TOOKAD®), phthalocyanines (phthalocyanine 4 (Pc4)) and texaphyrins (Lutex®) (10). In this study, the photosensitizer is a porphyrin compound (Figure 4). Porphyrins are large molecules which make it possible to have one part of the molecule be polar while another part is non-polar (7). Following endocytosis of Photofrin® drug, the sensitizer molecules preferentially accumulate in the lipophilic compartments of tumor cells such as the plasma membrane and endoplasmic reticulum, but concentrations in the mitochondria are generally 1000-fold higher (8).

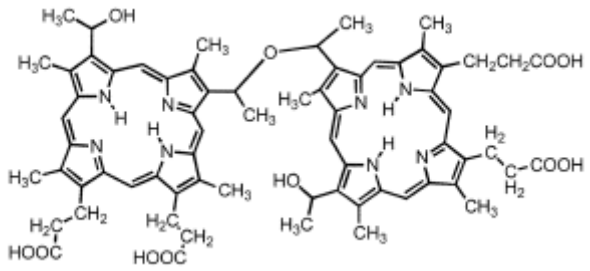

Figure 2. The FDA approved PDT drug: Photofrin® is a porphyrin molecule (10).

PDT kills tumor cells in a variety of ways. Directly, as described above, but PDT also damages the vasculature if the photosensitizer is still in the vessels when light treatment occurs. In addition, PDT activates the immune system through localized inflammation. Studies of mRNA and protein expression before and after PDT treatment have shown that PDT causes upregulation and downregulation of many proteins. PDT-mediated oxidative stress induces an upregulation of early response genes c-fos, c-jun. c-myc and egr-1 (2) inducing cellular responses promoting apoptosis. Not surprisingly, based on the cellular insult of PDT, multiple genes encoding stress-induced proteins are also activated post-PDT treatment. These include heme oxygenase and heat shock proteins (11). In addition to these proteins, PDT activates other factors important in immune function such as interleukin-6, interleukin-10, and nuclear factor kappa B (2). Enhanced expression of early response genes and stress proteins works to activate the immune system affecting functions such as cell adhesion, antigen presentation and inflammation (2).

PDT is currently used to treat a variety of cancers and has the potential to treat several others. PDT is the favored treatment of Barrett's esophagus because of its treatment benefits and economical factors. Although prognosis for lung cancer is

often poor, PDT can be used for this type of cancer, increasing survival and/or improving quality of life for the patient. A Japanese clinical study using PDT on lung cancer has shown promising results: complete response in 84% of patients and partial response in 15% with tumor recurrence in only 11% of complete and partial response patients combined (13). PDT can also be used in conjunction with other therapies such as surgery. If a lung tumor is inoperable at presentation, PDT can be used to shrink the tumor and convert it to an operable one (12). PDT has been used for gastrointestinal cancers for over 20 years, debulking tumors as a palliative care measure. PDT could be used on inoperable brain tumors giving patients a more favorable prognosis. Based on mouse studies, PDT has a promising future in treating malignant melanoma as well as non-melanoma skin cancer (12). Studies are underway evaluating PDT's success at treating eye diseases such as choroidal melanoma and other intra-ocular tumors (12). Described here are just a few examples of the uses of PDT. PDT has the potential to treat many types of cancers as a primary treatment, in conjunction with other treatment methods, or as palliative care to improve the quality of life for a cancer patient. Some interesting clinical trials are underway to increase the success of bone marrow transplantation in acute leukemia and non-Hodgkin's lymphoma patients. Bone marrow transplants to these patients often result in relapse because of tumor cell contamination. To help decrease the instances of relapse, trials are testing PDT to eliminate tumor cell contamination of the marrow. This method does not involve introducing toxic chemical agents or

foreign antibodies that would induce immune activation and prejudice the transplant survival (12).

PDT has a promising future in cancer treatment. However, because of its many benefits, it is also being studied as a treatment for other types of diseases. Rheumatoid arthritis, psoriasis, and many eye diseases including age-related macular degeneration (12) are a few examples of common and debilitating diseases that are or could be treated with PDT. In addition, PDT can be used to treat infectious disease. The number of antibiotic resistant strains of bacteria is increasing rapidly so the need to find alternative treatment options is vital. Studies are underway to treat localized infections of Methacillin-resistant *Staphylococcus aureus* and vancomycin-resistant enterococci (10). The photosensitizers used to treat infections would be applied topically and have different molecular frameworks to those used to treat cancers (10). Photosensitizers used to treat infectious diseases include halogenated xanthenes (Rose Bengal), phenothiazines (Toluidine Blue O and Methylene Blue), acridines and perylenequinones (hypericin) (10). These photosensitizers have a low dark toxicity to mammalian cells but when localized and activated are lethal to bacterial cells, especially Gram (+) species (10). The same treatments options exist for other microorganisms, viruses, fungi and yeasts (10).

There are numerous benefits of using PDT treatment; however, this treatment method does have its limitations. A PDT set-up can be expensive. Some types of lasers are expensive pieces of equipment that are very specific and do not really allow the flexibility of using a variety of sensitizers since each is excited by a specific

wavelength. The light sources used clinically at this time do not operate in the near infrared (NIR) tissue transparency window, so the treatment is limited to lesions that are within 1 mm of the body surface. Two side effects that have limited the use of PDT are nonspecific biodistribution and prolonged retention in tissue that forces patients to avoid light for many weeks after treatment (9). Another limitation of PDT is that it cannot be used to treat metastatic disease because it is not possible to irradiate the entire body in a reasonable time frame (6). These restrictions can be dealt with as further research reveals better targeted and faster clearing photosensitizers and more effective timing of drug injection to light irradiation.

History of Photodynamic Therapy

In 1900 a German medical student named Oscar Raab discovered that light at a certain wavelength in combination with the chemical acridine was lethal to *Paramecium caudatum* (4). The first recorded case of using this method to treat a cancer was three years later when H. von Tappeiner and A. Jesionek treated mice with basal cell carcinoma with topically applied eosin and white light (5). One year later, the method of using chemicals and light was coined "photodynamic action" (4). The treatment was first tested on a human in 1912 when German scientist F. Meyer-Betz injected himself with 200 mg of hematoporphyrin and experienced pain and swelling of his skin after light exposure (4). In 1942, H. Auler and G. Banzar discovered that porphyrins exhibited a modest preferential accumulation in tumor tissue when tested on rats (4). The selection was only about 3 times that of normal tissue (45). Throughout the years photosensitizers have evolved to become more

potent and better “targeted”. In 1960, R. L. Lipson and S. Schwartz observed that injections of hematoporphyrin led to fluorescence of neoplastic lesions. These scientists also treated hematoporphyrin with acetic acid to obtain a mixture called “hematoporphyrin derivative” (HPD) that was better at localizing in the tumor tissue and could be used for tumor detection (2). This HPD was purified and termed Photofrin® (2).

Photofrin®, the first generation photosensitizer, has spearheaded the current and future directions of PDT (Figure 2). The first country to approve Photofrin® was Canada in 1993, for treatment of bladder cancer. Closely following this, were The Netherlands and France, for treatment of advanced lung cancers (2). After clinical trials in Japan from June 1989 to March 1992, the Japanese government approved Photofrin® to treat early stage lung cancer in 1994. Japan was followed by Germany. Many more countries in Europe quickly followed suit. Photofrin® was approved as the first PDT drug by the United States FDA in 1995 to treat patients with high grade dysplasia in Barrett’s esophagus, and then in 1998 for patients with non-small cell lung cancer (2, 3). An advantage that Photofrin® had over the earlier photosensitizers was that it was activated by light at 630 nm and thus could penetrate moderately well into the tissue, especially compared to topically applied eosin (5). In addition, Photofrin® accumulates moderately well in the mitochondria of tumor cells. However, Photofrin® does not clear from the body quickly, and skin photosensitivity persists for four to 12 weeks after treatment (5, 14). Photofrin® has been a great starting place for clinical use of PDT; however, the ideal photosensitizer should be

chemically pure and of known specific composition (this is especially significant for toxicity testing), have a high quantum yield for singlet oxygen production, have a strong absorption at a long wavelength (for maximum tissue penetration), have excellent photochemical reactivity, have minimal dark toxicity, and only be toxic in the presence of the correct wavelength of light (4). The ideal photosensitizer should also have strong preferential accumulation and retention in tumor tissue, clear rapidly from the patient's body after treatment, and be easy to synthesize and give to a patient intraveneously (4).

In order to try to fulfill these requirements, a wave of second generation of photosensitizers was created. Among these are Benzoporphryn Derivative (BPD) which has a strong absorption at 692 nm and it is cleared from the body quite rapidly through the feces. However, BPD is only somewhat selective in tumor accumulation (14). Aminolevulinic acid HCl (ALA) (Levulan®) received approval in 1999 (5) and is currently used to treat acne and other skin lesions. In the mitochondria, 5-aminolevulinic acid is formed during the first step of the heme biosynthetic pathway from glycine and succinyl-CoA (60). The last step of the pathway is the incorporation of iron into protoporphyrin IX (PpIX), a compound that possesses properties of an efficient photosensitizer (64). With the addition of exogenous ALA, PpIX accumulates with some degree of selectivity and, with light application, PDT can take advantage of this endogenous photosensitizer (64). ALA treatment differs from the other photosensitizers discussed because it uses an endogenous photosensitizer. Other PDT drugs discussed herein are considered exogenous

because the photosensitizer comes from a drug that is administered, not a substance produced in cells. ALA's biggest advantage is its rapid clearance of only 1-2 days, but it is water soluble thus not able to enter cells well (5). Meta-tetra(hydroxyphenyl)chlorine (mTHPC) (temoporfin or Foscan®) is the most recent photosensitizer to gain approval for use. It was approved in 2001 in Europe for the palliative treatment of head and neck cancers. The absorption wavelength of mTHPC is 652 and photosensitivity post-treatment only lasts 2-4 weeks (5). Another second generation photosensitizer is known as WST09 or Tookad®. Tookad® is a palladium-metalated bacteriopheophorbide that is activated at 763 nm (15). Treatment with Tookad® targets the tumor vasculature making the "drug to light" interval very short, so that the photosensitizer is still contained within the vessels upon activation (15). Tookad® is only retained in tissue for three hours post treatment (15). These second generation photosensitizers all have a longer absorption wavelength for increased tissue penetration. Bis-amino (IV) phthalocyanine (BAM-SiPc) is another second generation photosensitizer. It is a potent photosensitizer that leads to tumor cell death through the apoptotic pathway (9). However, the biodistribution and localization problems of BAM-SiPc may inhibit its clinical use (9).

As second generation sensitizers are tackling the flaws of their prior generation, third generation photosensitizers are coming to the forefront doing the same for the second generation sensitizers. Third generation sensitizers are not only improving tissue penetration and drug clearance, but also improving targeting to

increase selective affinity of the photosensitizer for the tumor tissue (9). Targeting moieties, such as single-chain monoclonal antibodies, will enable the sensitizer to kill tumor cells while minimizing healthy cell damage (9).

PDT and the Immune Response

Most of the common cancer therapies are immunosuppressive. The doses required for chemotherapy and radiation to be effective are toxic to bone marrow, the source of cells of the immune system (16). Major surgery can also have immunosuppressive effects demonstrated by reduced cellular proliferation and reduced secretion of interleukin-2 (IL-2) and gamma interferon (IFN-γ) by mitogen-stimulated T lymphocytes (65). The decreases in cell proliferation and IL-2 production, but not IFN-γ production, appear to be the result of inhibitory factors, such as prostaglandin E2 that are released from mononuclear phagocytes at elevated levels after injury (65). In addition, alterations of monocyte functions have been reported after major surgery, including loss of cell surface human leukocyte antigen-dr (HLA-DR) molecules as well as reduced secretion of cytokines, including IL-1, IL-6, and IL-8 (65). The ideal cancer therapy would not only be able to kill the primary tumor, but activate the immune system to recognize, find and destroy any residual or metastatic tumor cells. PDT-induced anti-tumor immunity was first demonstrated by Canti *et. al*. when he showed mice treated with PDT were resistant to subsequent tumor challenges, and that cells isolated from tumor draining lymph nodes from PDT treated mice could be transferred to naïve mice and carry with them this tumor

resistance (18). A separate study confirmed this finding, and found that anti-tumor immunity resulting from PDT treatment was very active 40 days post-treatment (20).

The photooxidative lesions from a treatment session are recognized by the immune system as altered self. Altered self activates the complement component of the innate immune system. Complement is engaged by one of three pathways: classical, alternative or lectin mediated, in response to pathogens, foreign cells, or cells of the body that are altered and no longer recognized as self (17). Complement opsonized cells that have undergone PDT treatment then attract neutrophils, monocytes/macrophages, dendritic cells, and other immune cells displaying complement receptors (17, 19) (Figure 3). Neutrophil infiltration at the tumor site is essential for an immune response (21). Post-PDT treatment activated neutrophils can remain within tumor vasculature causing endothelial cell damage which releases cytokines and chemokines that will attract a fresh wave of immune cells (19, 17). In addition, macrophages and dendritic cells are attracted to the tumor site and phagocytosis of cancer cells occurs to generate antigen presenting cells. They present tumor specific antigens to major histocompatibility class II molecules (19). The presentation causes T lymphocytes to recognize and destroy tumor cells (19, 22); one study found that this is the action of CD8(+) T cells, in particular (20). Since neutrophils are so important in initiating the immune response, high levels of neutrophils infiltrating the treatment site may serve as a positive clinical prognostic indicator (21).

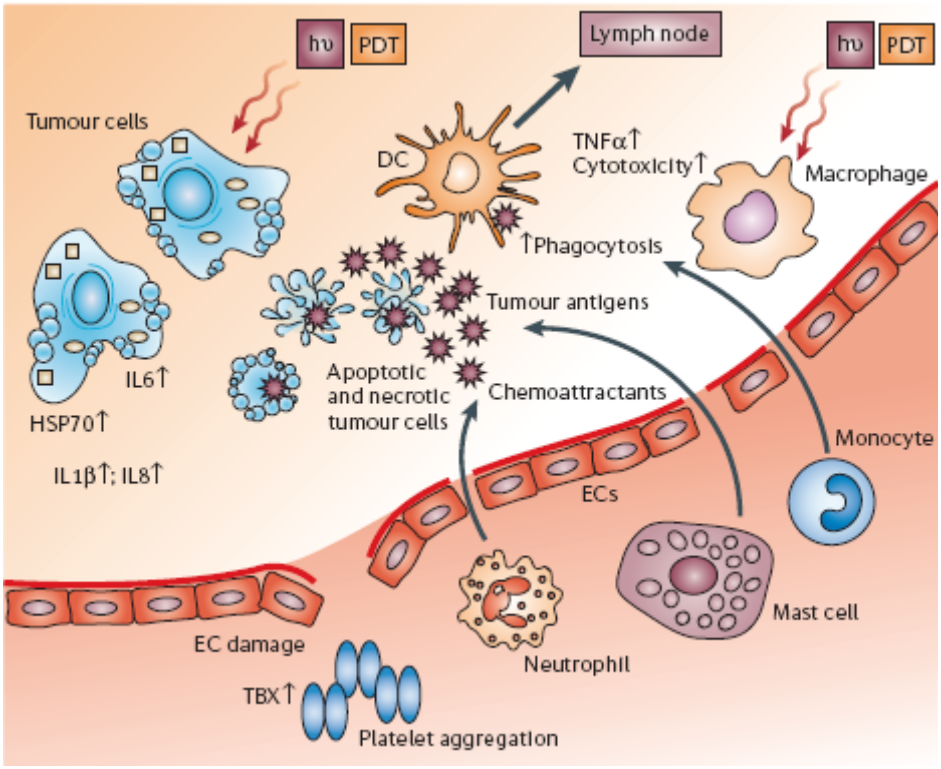

Figure 3. PDT induced activation of antigen specific T cells (16). Endothelial cell damage and tumor cell death leads to inflammation, neutrophil infiltration, chemokine and cytokine release and infiltration of immune cells. Figure used with permission from the author and the Nature Publishing Group (NPG).

Immune activation from inflammatory and immune responses are key contributors to the efficacy of PDT treating cancer (17). In fact, complete tumor resolution after PDT treatment requires immune activation and function (19). PDT-induced immune activation presents another aspect where PDT could be used as an adjuvant therapy, possibly with a drug that also activates the complement system to enhance the immune activation.

Cancer

In the year 2007, 1,444,920 people were diagnosed with cancer; another 1,437,180 people are expected to be diagnosed with cancer in 2008 (23). This year 565,650 Americans are expected to die of cancer, that is 1,500 people each day (23). Cancer is the second most common cause of death in the US led only by heart disease, and one in every four deaths was due to cancer (23). The overall cost of cancer in 2007 was 219.2 billion dollars including costs for medical care and loss of productivity (23).

The two types of cancer used in the current study were breast and lung. Of the 1,444,920 people expected to be diagnosed with cancer this year, 184,450 cases are expected to have breast cancer and 40,930 breast cancer patients are expected to die (23). Breast cancer patients are usually women but occasionally can be men. Risk factors for breast cancer include early menarche, never having carried a baby, age, personal and family history (5% - 10% of people have a germline mutation of BRCA 1 and BRCA 2 genes) (23). There are many treatment options depending on the size of the tumor, type of cancer cells and stage of cancer progression. One treatment choice is a lumpectomy which saves as much of the breast as possible, but this treatment is limited to smaller tumors, and is often followed with radiation to kill any cancer cells not removed by surgery. There are various types of mastectomy. A partial or segmental mastectomy removes the tumor and some breast tissue along with the fascia under the tumor. A segmental mastectomy saves much of the breast, but it is often followed by radiation treatment (24). A simple mastectomy procedure

removes all the breast tissue, and is usually followed by treatments of radiation, chemotherapy or hormone therapy (24). A radical mastectomy consists of removing the breast, lymph nodes and chest muscles, but is rarely done now because the procedure is so invasive and deforming. In addition, many problems follow a radical mastectomy such as lymphodema and a high risk of infections. A modified radical mastectomy is quite common and removes the entire breast, overlaying skin and underarm lymph nodes (24). The first tumor draining lymph node is the sentinel node, and a sentinel lymph node biopsy is common. If cancer cells are found in the sentinel lymph nodes, these nodes are removed along with the axillary lymph nodes to prevent further cancer spread (24). Breast reconstruction often follows mastectomies. Other treatment options include radiation, chemotherapy, hormone therapy and biological therapy. Radiation is used commonly after surgery to ensure as much cancer cell kill as possible. It is also used for cancer that has invaded the chest wall or that has spread to more than four lymph nodes in the axilla (24). Side effects are unpleasant including lymphodema of the arm, damage to lungs, heart or nerves, change in the breast tissue and an increased risk of developing another tumor (24). Chemotherapy is used to decrease the chance that cancer will recur, to try and control the spread of the disease, or to ease any symptoms the cancer mass is causing (24). However, chemotherapy can cause hair loss, nausea, vomiting, fatigue, damage to the heart, nerves, kidneys, and other organs, damage to immune cells, "chemobrain" a condition that causes memory and concentration problems, premature menopause and infertility (24). Hormone therapy works to decrease the chance of the

cancer returning and to reduce the tumor burden (24). There are two types of hormone therapy. Selective estrogen receptor modulators (SERMS) block endogenous estrogen from attaching to receptors on cancer cells, slowing tumor growth and killing cancer cells. An example of this type of drug is Tamoxifen (Nolvadex) (24). The second type of hormone modulators are the aromatase inhibitors that stop estrogen production in cells other than the ovaries. Examples of this type of drug include anastrozole (Arimidex), letrozole (Femara), and exemestane (androstenedione) (24). These drugs increase the risk of osteoporosis and only post-menopausal women are eligible. Biological therapies take advantage of proteins such as HER2-neu that are overexpressed on tumor cells or other proteins that are overexpressed on tumor vasculature. These treatments use monoclonal antibodies to block receptor sites and kill cells. Lapatimb (Tykerb) is approved to use in conjunction with chemotherapy in women with advanced metastatic breast cancer (24).

Of the 1,437,180 new cancer cases diagnosed in 2008, 215,020 cases are expected to be lung cancer (23). Lung cancer usually forms from the cells lining air passages. The two main types are small cell lung cancer and non-small cell lung cancer and they are characterized by the size of the cell when viewed under the microscope (23). Small cell lung cancers (SCLC) are less common, grow very quickly, and have often already spread to other parts of the body by the time the cancer is diagnosed (24). Non small cell lung cancer includes adenocarcinoma, the most common type of lung cancer (30 – 40% of cases) and squamous cell carcinoma,

the second most common type of lung cancer (30% of cases) (24). It is estimated that 161,840 people will die from lung cancer this year (23). Lung cancer is the leading cause of cancer deaths among Americans (24). Risk factors include smoking, exposure to second hand smoke, radiation therapy of the breast or chest area, occupational hazards such as asbestos, radon, arsenic, soot, tar, exposure to air pollution (25). An additional risk factor emerging for lung cancer is genetics (66). Studies have shown that two single nucleotide polymorphisms (SNP) on chromosome 15 increase the likelihood of developing lung cancer by 28-81% (66).

Treatment options include surgery, radiation, chemotherapy, and PDT (24). The option a patient and his or her doctor select depends on if the type is small cell versus non-small cell, tumor stage, and the patient's general physical condition (23). Surgery can range from minimally invasive to major. A thoracoscopy is a way to access the chest through small incisions to diagnose and treat cancer (24). The other surgery treatment options are more invasive because they require a major chest incision to get to the lung tissue. These treatments range from a wedge resection (removing a small section of the lung) to a lobectomy (removing an entire lobe of one lung) to a pneumonectomy (removing an entire lung) (24). Radiation can be a treatment option alone or with surgery. PDT using Photofrin® and a light delivered using a bronchoscope is also a treatment option (24). Radiation, chemotherapy, and PDT all have undesirable side effects as mentioned earlier.

Two-Photon Photodynamic Therapy

A major limitation of the current PDT treatments available is that the light used is not able to penetrate any distance into the tissue, so only surface lesions and lesions that can be reached using a scope are eligible for PDT treatment. This is because the absorption of visible light in the tissue is high and this light scatters a great deal in biological tissues (26). Two-photon (2PA) PDT was first proposed in the 1930's by Maria Goppert-Mayer, but difficulty developing a suitable photosensitizer, and the requirement for expensive, large laser equipment, meant that 2PA PDT failed to attract a lot of attention until the 1960's. Two-photon PDT is now an emerging and promising specialty (26, 27). 2PA is a nonlinear optical process in which two photons are absorbed simultaneously, and, by combining their energies, promote the molecule to an excited state (26). 2PA porphyrin compounds can generate singlet oxygen at much longer light wavelengths, about 800-1000 versus 400-700 of one photon compounds. Longer wavelengths are in the tissue transparency window allowing for much better depth efficacy (26). In addition, 2PA excitation requires a much higher power density than one photon so the laser beam is more focused and consequently the laser can precisely illuminate only the area being treated (26). In 1997 two studies were published demonstrating the near infrared (NIR) excitation of a photosensitizer using a Ti: sapphire laser (26). These studies used 9, 10-anthracenedipropionic acid (ADPA), an established singlet oxygen scavenger in aqueous solutions. It reacts with singlet oxygen producing endoperoxide

and bleaching, and was used to show that 2PA did cause singlet oxygen production (26).

Another limitation of the current PDT drugs is poor targeting. Second and third generation sensitizers that use antibodies or large molecules to target the tumor run a high risk of being taken up in the liver and causing harmful immunological reactions (28, 29). Our novel 2PA PDT drug, RA 301, does not have those limitations (Figure 4).

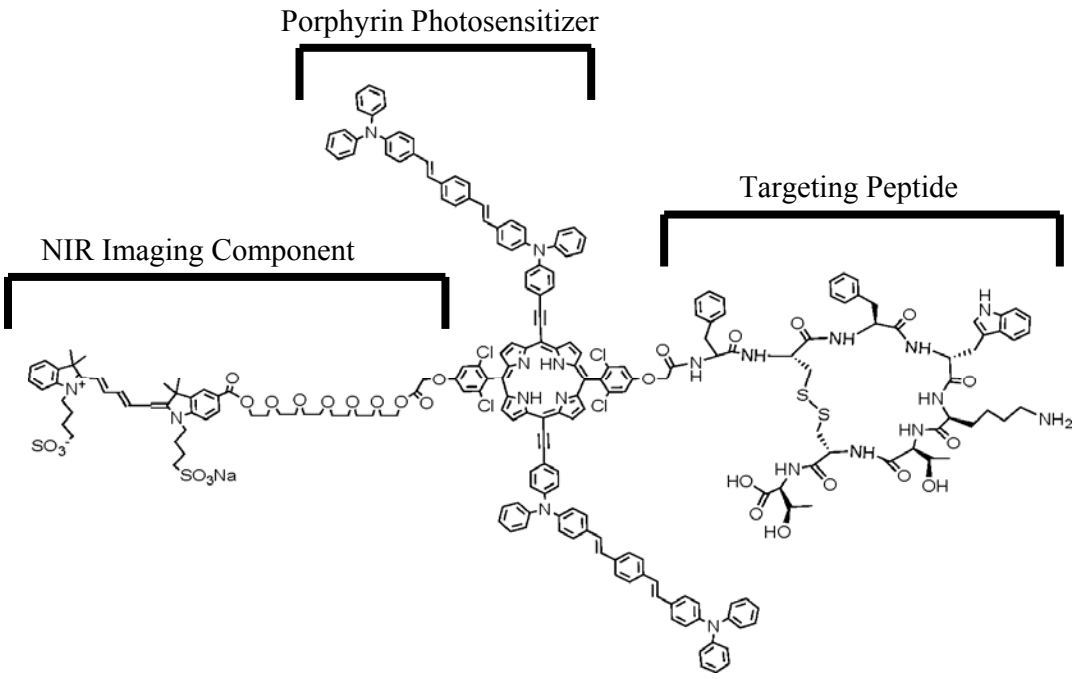

Figure 4. RA 301. RA 301 is consists of three moieties: the center portion is the porphyrin photosensitizer; the left is the NIR imaging component; and the right is the targeting peptide.

RA 301 takes advantage of the fact that many tumors overexpress the somatostatin receptor 2 (SSTr2) (Figure 4, component on the right). Somatostatin (SST) is a regulatory peptide hormone produced and secreted by neuroendocrine and inflammatory cells (30). It inhibits secretory and proliferative responses in target

cells by reducing the synthesis and secretion of local and systemic growth promoting factors (31). The biological effect of SST is mediated through a family of five specific high affinity G protein-coupled receptors (31). RA 301 is a 2PA PDT drug comprised of three components: a small peptide targeting the SSTr2 (Figure 4, right component), a NIR imaging agent to see *in vivo* where the drug is (Figure 4, left component), and a porphyrin that is activated by light in the tissue transparency window (Figure 4, center component) (28). Not only is SSTr2 overexpressed in a large percentage of tumors, but the SST analog octreoate is easy to obtain commercially. Octreoate is a SST analog that can mimic the biological actions of SST. SST analogs are used to treat growth disorders such as acromegaly and treat various endocrine tumors because they can bind to receptors as SST would and inhibit the action of growth hormones (32).

RA301 is moderately soluble in the Solutol® excipient (BASF), and is given to mice through tumor infiltration. In larger animals, the injection would be given intravenously. This is because Solutol is very viscous and the dose needed to be effective cannot be diluted enough for intravenous injection due to the small blood volume of mice. Once in the body, the drug will accumulate only in the tumor cells that are overexpressing somatostatin receptor 2. The deepest effective penetration of our PDT protocol is not known because all animal work has been done using mice that have a maximum body depth of about 2 cm. However, work in tissue phantoms has shown cell kill at 4 cm deep (28). In experimental mice, RA 301 has been shown to be cleared from the body after 24 hours (29). This drug is designed to solve

several of the problems of current PDT photosensitizers such as tumor cell targeting, using longer light wavelengths for increased depth in the tissue transparency window, and rapid clearance from the body after treatment.

Previous Experiment Leading into This Project

In vivo imaging is an important component of the projects done in the lab to observe what is happening to the tumor. In our lab, select cancer cell lines were transfected to express a luciferase gene. Luciferase is an enzyme used in the lab for bioluminescence assays. When luciferase expressing cancer cells form a tumor it is possible to visualize the cells using 0.02 ml of luciferin (1 mg/ 0.01 ml of PBS) injected intravenously. The luciferin causes the enzyme luciferase to undergo an oxidation reaction, producing light. It was observed through this type of *in vivo* imaging, carried out before and after PDT treatment, that the tumor exhibited a large amount of luciferase bioluminescence before PDT treatment and virtually none after treatment. This observation led us to wonder whether we had killed all the cancer cells and there were no cells left to express the bioluminescent signal. Or if there had been a shutdown of the tumor vasculature as a result of PDT treatment and the luciferin was not able to circulate to the tumor cells. The latter option was investigated in this project.

CHAPTER 2

MATERIALS AND METHODS

In vivo Octreoate Cell Binding Experiments

This set of experiments elaborated on the experiment that led into this project. They demonstrate the importance of our novel PDT drug binding to the somatostatin receptors on the tumor cells for its effectiveness.

Mice used in this entire study were CB17 *SCID*. All animal procedures were performed under general anaesthesia with inhaled isofluorane and were carried out according to the NIH Principles of Laboratory Animal Care and approved by the MSU Institutional Animal Care and Use Committee (IAUCAC).

The small cell lung cancer line, NCI H69, and the non-small cell lung cancer line, A549, were propagated in tissue culture. The cell lines were grown in 10 ml plastic cell culture flasks in DME/F-12 cell growth medium supplemented with 10% fetal bovine serum, 0.12% sodium bicarbonate, 0.10 μg/L insulin, and cover antibiotics. Cells were fed twice each week and when the cells reached a confluency of approximately 80-90% they were subcultured. Subculture was carried out by first removing spent cell medium and incubating the cells for 10 minutes at room temperature in Tyrodes $Ca^{2+}Mg^{2+}$ -free saline, followed by a brief incubation at room temperature in 0.05% Trypsin plus 0.02% EDTA. Adherent cells were rinsed off of the flask with 1 ml of serum containing cell medium, also stopping further trypsinization. One drop of new media plus cells was added to a new flask containing

10 ml of fresh medium. If, as in this case, the cells were needed for an experiment in high numbers, the cells were subcultured into two to four 50 ml flasks. In this experiment, both cell lines were needed to inject into mice to grow a tumor. As soon as the cells reached approximately 80-90% confluency the flasks were subcultured as described above, the cell suspension was added to a 50 ml plastic centrifuge tube and was centrifuged for seven minutes at 1000 rpm. For injection subcutaneously in mice, the cells were resuspended in complete medium at more than 10^7 cells per 0.1 ml/mouse.

The cell suspensions were kept on ice until injection. To grow tumors, 0.1 ml of suspended cells plus 0.1 ml of BD Matrigel® Matrix (BD Biosciences) were injected using a plastic 1.0 ml tuberculine syringe equipped with a 27 gauge needle. Lung tumor cells were injected subcutaneously in the flank region.

When the tumors reached about $1cm^3$ or after adequate blood vessels had formed for the tumor to be considered angiogenic the mice were anaesthetized and treated with Nair® to remove hair on and around the tumor. The next day the tumors were imaged to give a pretreatment baseline.

In vivo imaging was done by first injecting the mice intravenously via the tail vein with 0.2 ml (10 mg per ml, 2 ml per kg body weight) 150,000 - molecular weight (kilo Dalton) FITC dextran (34). This particular molecular weight dextran is large enough that it will remain within the vasculature until it reaches the leaky vessels of the tumor where it will extravasate within the tumor. An experiment to determine the time post injection in which the highest concentration of FITC dextran accumulated at

the tumor site had been carried out previously. Following this earlier data, the mouse was imaged at forty minutes post FITC dextran injection. Imaging was carried out using a Kodak 2000MM scanner and equipped with a 449-500 nm bandpass excitation filter and a 535 emission filter. Mice were scanned for 5 minutes. The data was recorded using Kodak scanner software.

Since this experiment was designed to determine the importance of the drug binding to somatostatin receptors on tumor cells for effective treatment, in one experimental group of mice the somatostatin receptors were blocked using the somatostain analog, octreoate (35). To block the receptors, 0.1 ml of octreoate (1 mg/ ml CMF) was injected intravenously just before PDT drug injection. The sensitizer (100-200 μg) was infiltrated into the tumor in PDT treated mice. Photodynamic therapy treatment was carried out on mice four hours after injection of the PDT drug. A 2-photon NIR laser beam was rastered through the entire tumor in approximately 20-30 minutes, depending upon the size of the tumor (28). The average pulse energy was measured at the tumor and was 847 mW at a 1 kHz pulse repetition rate. Pulse duration was ca, 150-200 fs as measured using an auto-correlator (28). The laser wavelength was 790 nm with a bandwidth of ca. 10 nm (28). During experimentation, the laser beam was focused with a spherical lens of focal length f = 400 mm (28). The distance between the lens and the tumor was 200 mm so the average density in the laser spot was ca. $5W/cm^2$ (28).

In vivo imaging after treatment was conducted in an identical manner to that used to establish the pretreatment baseline in order to observe what effect PDT had on

the tumor vasculature. In addition to *in vivo* imaging to determine the results for this experiment, the PDT effect on tumor volume was also measured and recorded. Tumors were measured daily using a ruler to observe the effect treatment has on tumor size. Tumor volume was calculated using the equation for the volume of an ellipse. The equation is $4/3\pi abc$ where a is radii front to back, b is radii side to side and c is radii top to bottom; all measurements were made in millimeters. There were four groups of mice used in this experiment: mice treated with octreoate and then PDT, mice treated with PDT, mice that were not treated in any way, and mice that were treated with octreoate only. Each group had four replicate mice. Data analysis was done after the experiment was completed by graphing the percent change in tumor volume against time.

Immunohistochemistry

Fluorescent immunohistochemical staining was carried out on tumor cell lines propagated in culture and tumor tissue from *SCID* mice to examine on a more in depth level what was happening to the tumor and tumor vascular tissue as a result of PDT treatment. Similar to the previous set of experiments, the somatostatin 2 receptor was the target of investigation since this is the receptor that the PDT drug targets. All imaging was done on a Leica® TCS-NT using a 63X 0.9 NA oil immersion objective, and either 488 nm or 568 nm laser excitation sources. Fluorescence filter combinations used for fluorescein dyes (green) were TD

488/568/633, RSP 580, BP 525/50, and for rhodamines (red) were the same but using a LP 590 instead of a bandpass emission filter.

Immunohistochemical
Staining of Tumor Cells in Culture

The breast cancer cell line, T47D, and the lung cancer cell lines, NCI H69 and A549, were grown in culture as described in the previous section. The MCF7 breast cancer cell line was also used in this study. Culture techniques for this cell line were identical to that described for other cell lines, except that these cells required the addition of 0.1% β-estradiol prepared at 10^{-5} M concentration to the medium. In this experiment cells were grown on glass coverslips. To prepare them, 1.5 mm coverslips were soaked in glacial acetic acid for 2 days. They were then taken out of the acid and rinsed with water seven times followed by a wash using 7X detergent. The coverslips were rinsed again using water seven times and then three times in DI water. The coverslips were stored until use in 95% ethanol. The clean coverslips were taken with tweezers and flamed to remove any remaining ethanol and placed in a 10 mm Petri dish, one coverslip per Petri dish. The Petri dish was filled with 3 ml of complete cell medium. When tumor cell cultures reached 80 – 90% confluency they were harvested as previously described. One drop of the suspended cells was added above the coverslip in each Petri dish. The cells were allowed to grow in a 7% CO_2 in air gassed 37°C incubator.

When cells reached 70-80% confluency they were used for staining. All the staining and rinsing steps took place in the Petri dish. To establish the best working

protocol for preserving and staining somatostatin receptors, we first determined which the best fixation technique was. Three fixatives were tested on T47D and MCF7 coverslip cultures: a) 100% ice cold acetone at 4°C for 10 minutes followed by air drying for 20 minutes, b) 75% ethanol and 25% acetone for 20 minutes at room temperature and c) 100% methanol for 20 minutes at room temperature. We also examined post-fixation after the primary antibody and detection steps. It was determined that acetone treatment before the antibody incubation was the best fixative. However, 100% acetone was a little harsh on the cells, and, for the rest of the experiments, we used acetone at a ratio of 75:25 in sterile DI water. Aldehyde fixatives were not used to avoid the problem of autofluorescence.

Although there were modifications made to the procedure depending on the specific experiment, the general method of staining cells on coverslips was as follows:

- Coverslips were rinsed two times with pre-warmed phenol red- free, serum-free DME/F12.
- Cells were fixed in ice cold 75% acetone to 25% water for 10 minutes at 4°C then air dried for 20 minutes.
- Coverslips were rinsed twice in PBS buffer (36) and then once in PBS containing 0.05% Tween 20 (36) (PBS-Tween).
- Cells were incubated in the primary antibody for one hour at room temperature. If a coverslip was not yet fixed it was incubated at 37°C in a 7% CO_2 in air gassed incubator.

- Coverslips were then rinsed three times with PBS-Tween.
- Cells were incubated in the secondary detection antibody for 30 minutes at room temperature. Again, if the coverslip was not yet fixed the cells were incubated in a 37°C gassed incubator. The coverslips were kept in the dark from this step on.
- Coverslips were rinsed three times with PBS-Tween, twice in PBS and twice in sterile DI water.
- If the coverslip was not yet fixed at this point, it was fixed as described above then rinsed twice in PBS-Tween, twice in PBS and twice in sterile DI water.
- Coverslips were mounted on slides using Prolong Gold Antifade (Molecular Probes).
- Cells were examined using a Leica® TCS-NT laser scanning confocal microscope equipped with a 63X oil immersion lens and the argon 488 laser line was used for excitation. Images were collected using the Leica® confocal software and MetaMorph®.

In this set of experiments, the primary antibody used was Rabbit Polyclonal anti-Somatostatin 2 Receptor (SSTr2) (Advanced Targeting Systems) diluted 1:250 (final working concentration was 4 µg/ml PBS) in 5% Normal Horse Serum; the detection probe was Protein A-FITC (Pierce) diluted 1:50 (final working concentration was 20 µg/ml PBS) in PBS- 0.05% Tween. The anti-SSTr2 antibody receptor was developed in a rabbit using a peptide corresponding to the extracellular domain of SSTr2 (Advanced Targeting Systems), therefore, membrane antibody binding is expected.

The Protein A-FITC works well as a detection agent because it binds to the Fc portion of the primary antibody, and it is a bright fluor. A negative control omitted the primary antibody.

The next experiment examined the ability of octreoate to block the antibody staining for the SST2 receptor. Four experimental groups were used: group 1 coverslips were treated with 1 ml of 100 μg octreoate/ml serum free media for 1 hour in a 37°C gassed incubator immediately after the fixation step, and were then stained for the SSTr2 as previously indicated. Group 2 coverslips were incubated in 0.50 ml of 100 μg/ml octreoate plus 0.50 ml of anti-SSTr2 primary antibody for 1 hour in a 37°C gassed incubator. Group 3 coverslips were incubated with the primary antibody, then incubated in 1 ml of 100 μg/ml octreoate and finally incubated in the detection agent. Group 4 coverslips were not incubated in octreoate at any time, but were stained for the SST2 receptor as described above. Any coverslip not being specifically treated during a particular step was incubated in PBS-Tween for that time period.

Tumor Tissue Preparation

Tumor cell lines, T47D, NCI H69 and A549, were grown in culture as described in the previous sections. In this experiment, the cells, once confluent in their culture flasks, were subcultured, suspended, and injected subcutaneously into mice as previously described. Lung cancer cells were injected subcutaneously in the flank region and breast cancer cells were injected subcutaneously in the area of the mammary fat pad. Tumors were allowed to grow until they were at least 1 cm^3. The

mice were sacrificed and the tumor was dissected out. The tumor was trimmed to only keep the areas that showed no signs of necrosis. The tissue was placed in a cryomold (TissueTek®) and embedded in OCT compound (optimal cutting temperature) matrix (TissueTek®) (37). The mold was placed in a petri dish and set to float in liquid nitrogen until completely frozen. Frozen tissue was stored in a -80°C freezer until needed.

When used for sectioning, the frozen molds were placed in the cryostat chamber at -20°C along with the blade for one hour. Tissue was sectioned into 10 μm sections (38) and picked up by melting onto a Superfrost Plus Gold slide. The slides containing sections were stored in a -80°C freezer until needed.

Immunohistochemical
Staining of Tissue Sections

The most successful steps from staining cells on coverslips were modified to create a protocol to stain tissue sections. Again, since somatostain 2 receptors are the target of our PDT drug they were focus of this investigation. The general staining procedure is as outlined below:

- Slides were taken out of the freezer the day before staining and set out to dry overnight at room temperature.
- Sections were fixed in 75% ice cold acetone and 25% water for 10 minutes at 4°C and then air dried for 20 minutes.
- Sections were washed three times in PBS and then twice in PBS-Tween.

- If kidney sections were used in the experiment, endogenous biotin was blocked at this point in the staining procedure. This was carried out as shown below:
    - 15 minutes at room temperature in 0.05% Biotin in PBS.
    - 15 minutes at room temperature in 0.05% Streptavidin in PBS.
    - Wash twice with PBS-Tween.
- Sections were incubated in the primary antibody in a hydration chamber for one hour at room temperature.
- Sections were rinsed three times in PBS-Tween.
- The primary antibody was detected by incubation in a fluorescent tagged Protein A for one hour at room temperature. From this step onward the slides were kept in the dark.
- Sections were washed three times in PBS-Tween, twice in PBS and twice in sterile DI water.
- If the experiment called for double staining the second antibody was applied, rinsed, and detected in the same manner as described elsewhere in this thesis.
- Coverslips were mounted on top of the tissue sections using Prolong Gold Antifade and left to dry.
- Tissue sections were examined using a 63X oil immersion lens on a Leica® laser scanning confocal microscope equipped with a 488 argon laser and a 568 krypton laser. The images were collected using Leica® confocal software and

MetaMorph® and adjusted to reduce background using Adobe® Photoshop software.

A blocking step for nonspecific antibody binding was not necessary because the tissue was taken from *SCID* mice that do not have endogenous antibodies. This assumption was tested using a 5% Normal Horse Serum blocking step, and no difference was seen in the staining results.

To begin, tissue sections were incubated with anti-somatostatin 2 receptor primary antibody diluted 1:250 (final working concentration was 4 µg/ml PBS) in PBS-Tween and detected using Protein A-FITC diluted 1:100 (final working concentration was 10 µg/ml PBS) in PBS-Tween. When imaged, it appeared that tumor vasculature was being stained. To be sure that it was vessels that were being stained the next set of tissue sections were stained using rabbit polyclonal anti-human vonWillebrand Factor (vWF) (Factor VIII) (Dako) diluted 1:100 (final working concentration was 10 µg/ml PBS) in PBS-Tween for 1 hour at room temperature as the primary antibody and detected using Protein A-FITC. vWF was used because it is a well established endothelial cell marker (43). To further prove that vessels were being stained by the anti-SSTr2 antibody, tissue sections were double stained for somatostatin 2 receptor detected with Protein A-FITC and for vWF detected with Protein A conjugated to Alexa Fluor 568 (Pierce). These staining procedures were completed on SSTr2- positive tumor cells, NCI-H69 (39) and T47D (39), and on SSTr2-negative cells, A549 (40). A negative control slide was used in each set of experiments. This slide was not incubated in primary antibody.

Octreoate Binding/Uptake Experiment

This set of experiments was designed to examine if endothelial cells of the tumor vasculature were taking up the PDT drug. These experiments could show if the octreoate targeted PDT sensitizer was targeting tumor vessels because the endothelial cells were expressing the somatostatin receptors.

Octreoate Conjugation

For this set of experiments octreoate needed to be conjugated to a material that could bind to a fluorescent marker. To do this we decided to take advantage of the extreme binding avidity avidin and biotin have for each other.

Avidin is an egg white glycoprotein. Avidin and its analogues streptavidin and NeutrAvidin (Molecular Probes) have a very high affinity for biotin (K_a is approximately 10^{15} M^{-1}) (41). NeutrAvidin is deglycosylated (41) and is advantageous to use in staining procedures because there is less positive charge on the surface of the molecule and the NeutrAvidin will not bind nonspecifically to negatively charged cell surfaces and nucleic acids as much (42). Avidins are mainly composed of β-pleated sheets and are tetramers of identical subunits each of which contains a single biotin binding site (41).

The first step was to biotinylate octreoate. This was done using EZ-Link® Amine-PEGn-Biotin (Pierce) (Figure 5). This is a water soluble biotinylation reagent that features a polyethylene glycol (PEG) spacer arm and a terminal primary amine.

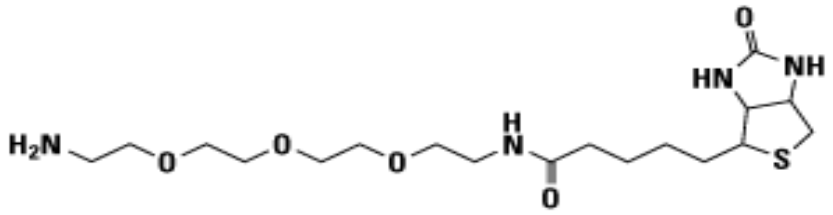

Amine-PEG3-Biotin
M.W. 418.55
Spacer Arm 22.9 Å

Figure 5. Amine-PEG_3-Biotin (Thermo Scientific)

The procedure followed to do this was recommended by Pierce. Fresh 2-(N-morpholino) ethanesulfonic acid (MES) buffer was made up by dissolving 70.4 g MES free acid monohydrate and 193.3 g MES sodium salt in 800 ml of molecular biology grade water. After mixing the volume was adjusted to 1000 ml and the pH was adjusted to pH= 5.78. Five-2 mg aliquots of octreoate were dissolved in 1 ml of MES buffer each. A 50 mM solution of Amine-PEG_3-Biotin was prepared by dissolving 21 mg in 1 ml MES buffer. Sixty µl of the Amine-PEG-Biotin solution was added to the dissolved octreoate and mixed (this resulted in the addition of 3 µmol Amine-PEG-Biotin, a 100-fold excess over octreoate to ensure binding). A 100 mM solution of 1-Ethyl-3-[3-dimethylaminopropyl]carbodiimide hydrochloride (EDC) (Thermo Scientific) was prepared in MES buffer by dissolving 19 mg in 1 ml of buffer. This was completed quickly because EDC is very sensitive to moisture. EDC works as a crosslinking agent to couple carboxyl groups to the $–NH_2$ group of the amine-biotin, forming an amide bond. Three µl of the EDC solution was added to the octreoate-Amine-PEG-Biotin solution and incubated for two hours at room temperature with constant mixing. The tubes were centrifuged to remove any

precipitate that was formed during the reaction, unreacted biotinylation reagent and any EDC by-products were removed by putting the mixture through a Bio-Gel P-GDG desalting column.

To determine if the reaction was successful the liquid collections from the desalting column were tested using an Immuno4 96-well plate and streptavidin conjugated to Alexa Fluor 488 (Pierce). To do this 100 µl of each fraction was added to one well of the 96-well plate. Non specific binding was inhibited using 180 µl of 5% Normal Horse Serum diluted in PBS incubated for 30 minutes at 37 °C. Wells were rinsed four times using 200 µl of PBS. Wells were then incubated with 90 µl streptavidin Alexa Fluor 488 diluted 1:100 (final working concentration was 10 µg/ml PBS) in PBS for 30 minutes at 37 °C. The streptavidin Alexa Fluor 488 was removed, and the wells were rinsed three times using 200 µl of PBS. Any remaining liquid was shaken out onto a Technicloth wipe and the fluorescent levels of the plates were checked on the Kodak Scanner equipped using excitation and emission filters appropriate for FITC fluorescence. Presence of the biotinylated peptide was confirmed by reading the fractions collected from the desalting column on a spectrophotometer. The desired wavelength was $\lambda = 214$ to monitor the presence of peptide bonds. Readings were taken of the MES coupling buffer, of blank tubes containing only water and of each fraction from the desalting column. From these readings the fractions were pooled into three samples. Sample 1, made up of the material from the fractions with the highest $\lambda = 214$ spec readings, was kept. Samples 2 and 3 were made up of the next highest and the lowest $\lambda = 214$ readings respectively

and were frozen in a -80°C freezer. Sample 1 was dialysized to remove any residual contaminants because the product was going to be used on live cells. This sample was added to 1000 kD cut off pore size dialysis tubing (Spectrum Labs) and placed into a 500 ml cylinder filled with a dilution of 1/30 PBS. Dialysis was conducted with constant stirring. Three changes of 1/30 PBS were made at 20 minute increments. The dialyzed product was frozen at an angle in a -80°C freezer and lyophilyzed overnight. The lyophilyzed product was reconstituted in 2 ml sterile DI water (10 ml biotinylated octreoate/ 2 ml water) and frozen in 250 µl aliquots.

Cell Staining
Using Biotinylated Octreoate

The breast and lung cancer cell lines, T47D and A549, were grown in tissue culture on glass coverslips as described in previous sections. Once the cells reached approximately 80-90% confluency they were ready to be stained. These cells were stained using a similar procedure to that described previously for staining cells on coverslips. In this experiment, however, the primary reagent was the biotin-conjugated octreoate diluted 1:100 in PBS-Tween and the cells were incubated in a 37°C gassed incubator for 30 minutes. Detection was carried out using NeutrAvidin Texas Red (Molecular Probes). The NeutrAvidin Texas Red was diluted 1:50 (final working concentration was 20 µg/ml PBS) in PBS-Tween and incubated with the cells for 30 minutes in a gassed incubator. In each set of coverslips, one was left to be fixed after the primary reagent and detection incubations. The coverslips were mounted on slides using Prolong Gold Antifade and left to dry before examination

using a confocal microscope equipped with a 568 krypton laser. Images were collected using Leica® confocal software and MetaMorph® software.

Octreoate binding/uptake experiments were also done on endothelial cells grown in culture. For this experiment, bovine aortic endothelial (BAE) cells were used. The cells were grown in culture in an identical manner as the tumor cell lines except that the medium consisted of Dulbecco's Modified Eagles High Glucose Medium (Sigma) plus 0.37% sodium bicarbonate, 10.0% fetal bovine serum, cover antibiotics, 0.01 μg/100 ml insulin, 100 μg/ml heparin, and 250 μg/ml endothelial cell growth supplement (Sigma). These cells were grown on glass coverslips, and stained in the same manner as the T47D and A549 cells. A negative control in all experiments omitted the octreoate incubation.

A second endothelial cell experiment was done to examine the effect of growth factors on octreoate binding. Bovine aortic endothelial cells were grown in culture on coverslips as described, except the medium in this experiment did not contain endothelial cell growth factor supplement. Four treatments were used in this experiment: a) one coverslip was grown in culture medium without added supplements; b) one coverslip was grown in medium that was taken off of A549 cells growing in the exponential phase in culture, filtered and mixed with an equal amount of fresh culture medium. Another c) coverslip was grown in culture medium supplemented with 10 ng/ml (46, 47, 48) murine vascular endothelial growth factor (VEGF) (PeproTech Inc). The last d) coverslip was grown in cell medium supplemented with 50 ng/ml (49, 50) recombinant human fibroblast growth factor

basic (bFGF) (R&D Systems). The cells were allowed to grow until 80-90% confluent then were stained following the same procedure described previously. The coverslip that was grown in unsupplemented medium was not only stained for SSTr2 using conjugated octreoate, but was also counterstained for polymerized actin using Alexa Fluor 488 Phalloidin (Molecular Probes) diluted 1:250 (final working concentration was 4 µg/ml PBS) in PBS-Tween for 30 minutes at room temperature. After staining, the cells were examined using a Leica® laser scanning confocal microscope equipped as previously described and images were collected using Leica® confocal software and MetaMorph® software.

Tissue Staining
Using Biotinylated Octreoate

To further examine the octreoate uptake in tumor cells and tumor vasculature the conjugated octreoate was incubated with tumor sections. NCI-H69 and A549 tumor cells were grown in culture and injected into *SCID* mice as previously described. Once the tumors were of appropriate size, they were dissected out and flash frozen as previously described. The frozen tumors were sectioned into 10 µm sections using a cryostat at -20°C and picked up onto Superfrost Plus Gold slides. To stain the tissue sections, the slides were taken out of the freezer the night before and allowed to air dry at room temperature. The staining procedure was similar to that of staining tissue sections as previously described except that, in place of the primary antibody, biotinylated octreoate was used. Tissue sections were incubated in biotinylated octreoate diluted 1:100 in PBS-Tween for one hour at room temperature

in a hydration chamber. Detection was carried out with an incubation in NeutrAvidin Texas Red diluted 1:50 (final working concentration was 20 μg/ml PBS) in PBS-Tween, also for one hour at room temperature in a hydration chamber. Half the slides were fixed before the application of the biotinylated octreoate and NeutrAvidin Texas Red and half the slides were fixed after biotinylated octreoate and NeutrAvidin Texas Red applications. The negative control slide omitted the incubation in biotinylated octreoate.

The final two sets of experiments were designed to prove that tumor vessels were binding octreoate. The first set of experiments was a double staining using biotinylated octreoate detected with NeutrAvidin Texas Red followed by a counterstain: Alexa Fluor 488 Phalloidin. This method allowed for better visualization of the vessels and the cells because it stains the polymerized actin of the cytoskeleton (44). The staining procedure was the same as the procedure already described for double staining tissue sections, with minor changes. One group of slides was fixed and incubated in biotinylated octreoate prepared as already described. The slides were then stained with NeutrAvidin Texas Red prepared as stated and counterstained using Alexa Fluor 488 phalloidin diluted 1:250 (final working concentration was 4 μg/ml PBS) in PBS-Tween for one hour at room temperature. A second group of slides was fixed, stained with Alexa Fluor 488 phalloidin, and then stained with biotinylated octreoate and NeutrAvidin Texas Red. The third group was incubated in biotinylated octreoate and NeutrAvidin Texas Red then counterstained and fixed last. The fourth group of slides was first counterstained

followed by the biotinylated octreoate and NeutrAvidin Texas Red staining and fixed very last. The control slide was only incubated with NeutrAvidin Texas Red.

The second set of experiments were also done on NCI H69 and A549 tissue sections and was also designed to ensure tumor vasculature was being labeled using the biotinylated octreoate. These experiments utilized vWF as an endothelial cell marker. The procedure was similar to one previously described for double staining tissue sections. Five groups of slides were used. Group 1 was fixed, incubated in biotinylated octreoate and NeutrAvidin Texas Red, and then incubated in anti-vWF diluted 1:100 (final working concentration was 10 μg/ml PBS) in PBS-Tween for one hour at room temperature in a hydration chamber. vWF was detected by another one hour incubation in Protein A conjugated to an Alexa Fluor 568 diluted 1:50 (final working concentration was 20 μg/ml PBS) in PBS-Tween. Slides in group 2 were fixed, incubated with anti-vWF and Protein A-568 and then incubated with biotinylated octreoate and NeutrAvidin Texas Red. Group 3 slides were first incubated in biotinylated octreoate and NeutrAvidin Texas Red followed by anti-vWF and Protein A-568 and fixed last. Slides in group 4 were stained with anti-vWF and Protein A-568 first, then in with biotinylated octreoate and NeutrAvidin Texas Red and, finally, fixed. The last group was fixed and stained with anti-vWF and Protein A-568 only.

CHAPTER 3

RESULTS

Results from the studies described in the previous chapter are presented in the same three section format. Each section focuses on a set of experiments highlighting somatostatin 2 receptor's role in PDT upon the cancer cells, the tumor vasculature and PDT's mode of action.

Experiments using an *In Vivo* Octreoate Block

These experiments used the somatostatin analog, octreoate, to block the somatostatin 2 receptors on the cells to prevent the PDT drug from binding. The evaluation of this experiment focused on the effect PDT had on the tumors when the targeted receptors were blocked versus not blocked.

The first mode of evaluation was done using 150,000- molecular weight FITC dextran to image the leaky tumor vasculature before and after PDT treatment. Mice from two experimental groups were imaged (Figure 6).

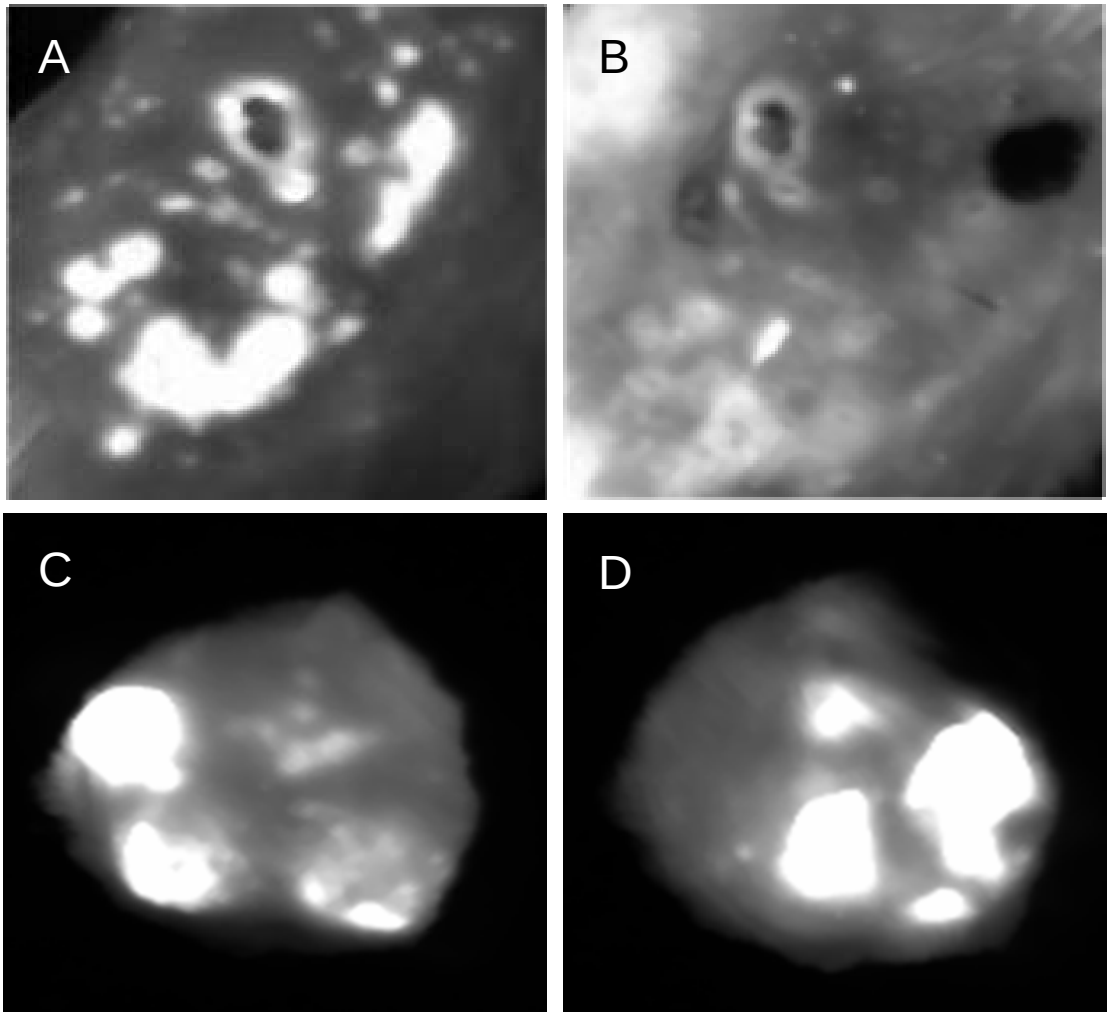

Figure 6. Images of lung tumors taken *in vivo* following an intravenous injection of high molecular weight FITC dextran. Images A and B were taken before and after PDT treatment, respectively. Images C and D were taken before and after PDT treatment, respectively; however, the mouse in this set of images received an injection of octreoate prior to PDT drug administration.

The image sets in Figure 6 (A and B versus C and D) show a striking difference in fluorescence intensity. The lack of fluorescence after PDT treatment in Figure 6b compared to the image taken before PDT treatment (Figure 6a) indicates that the FITC dextran was not able to circulate to the tumor indicates that the PDT is having an effect on the tumor vasculature. The images in Figure 6c and Figure 6d

demonstrate a requirement for SST2 receptor binding in generating this vascular effect. The fluorescence before and after treatment from the mouse that received an injection of octreoate prior to the PDT sensitizer, is similar, indicating that, in this case, PDT did not effect the tumor vasculature. These images demonstrate the importance of the PDT drug's ability to bind to the targeted receptors to cause vasculature shutdown.

The second mode of evaluating the experimental octreoate block was to follow the tumor growth rates. Tumor measurements started one day prior to PDT treatment and continued until the tumors got too large for the mice to be maintained on ethical grounds. The data was recorded as the percentage of growth as compared to the initial volume against time. Figure 7 below presents the results from both experimental replicates.

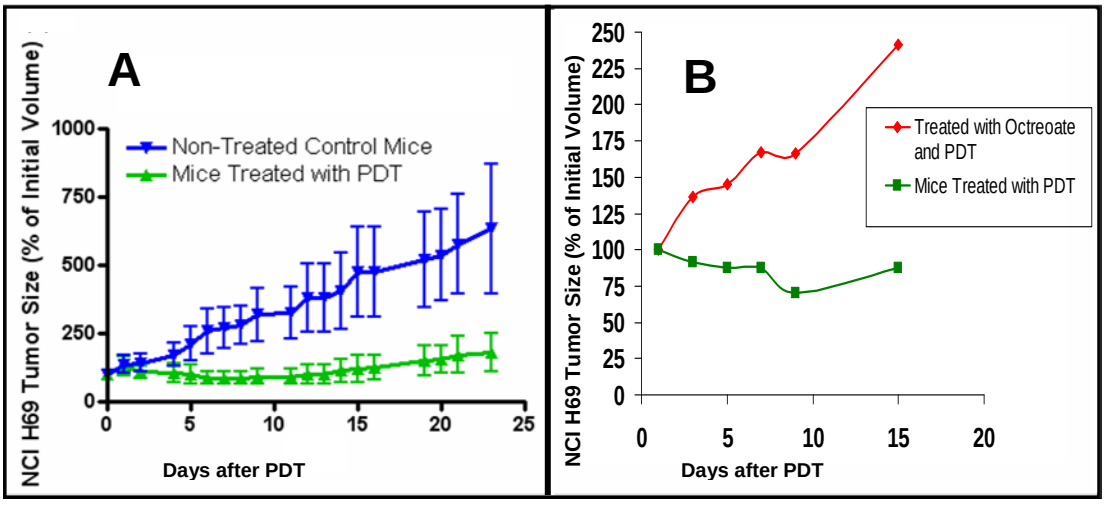

Figure 7. Results of evaluating tumor growth rates post PDT treatment. Panel A depicts NCI H69 tumors of two groups of mice. The first group (blue) was not treated. The second group (green) was administered the PDT drug and treated. Panel B depicts NCI H69 tumors of two additional groups of mice. The first group (red) was injected with octreoate followed by administration of the PDT drug and PDT treatment. The second group (green) was administered the PDT drug and treated.

These graphs demonstrate the effectiveness of PDT. Mice treated with PDT experienced tumor shrinkage followed by very little, slow tumor growth. However, mice that received no treatment or a treatment of octreoate followed by PDT exhibited rapid and extensive tumor growth. These data show that an octreoate block in the tumors will decrease the PDT effect by being in direct competition for SSTr2 binding sites.

Immunohistochemistry

Immunohistochemical Staining of Tumor Cells in Culture

Considering that staining for SST2 receptors was a new procedure in our laboratory, an effective staining protocol needed to be developed. The first step was to determine a fixation method that would preserve the SST2 receptors best. Three staining methods were tested as mentioned in the previous chapter.

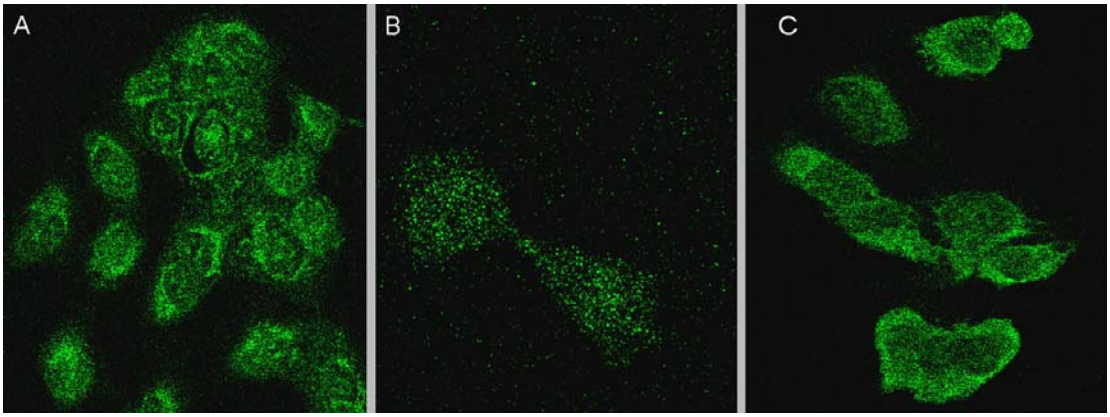

Figure 8. T47D cells grown on coverslips and stained for the somatostatin 2 receptor using Rabbit Polyclonal anti-somatostatin receptor 2 followed by detection using Protein A-FITC. Panel A depicts cells fixed using acetone at 4°C for 10 minutes and air dried for 20 minutes at room temperature. Panel B depicts cells fixed using 75% ethanol and 25% acetone for 20 minutes at room temperature. Panel C depicts cells fixed using methanol for 20 minutes at room temperature. These are single scan confocal images taken at the plane of best resolution.

These images in Figure 8 show the results of the different fixation trials. Acetone and ethanol (Figure 8b) was not considered a good fixation technique because it did not preserve the morphology of the cells well. Methanol (Figure 8c) seemed to preserve the staining of the receptors on the cell surface, but not as well as acetone (Figure 8a). In addition, cells fixed using acetone retained a more organized intracellular structure. However, 100% acetone was considered too harsh because, when the ice cold 100% acetone was added to the cells, many detached from the coverslip. Therefore, 75% acetone was used as the fixative for our studies.

Another aspect of the staining technique that needed to be tested was the order of fixation and staining. Fixation before and after anti-somatostatin 2 receptor antibody staining was tested on T47D and MCF7 cells as shown below in Figure 9.

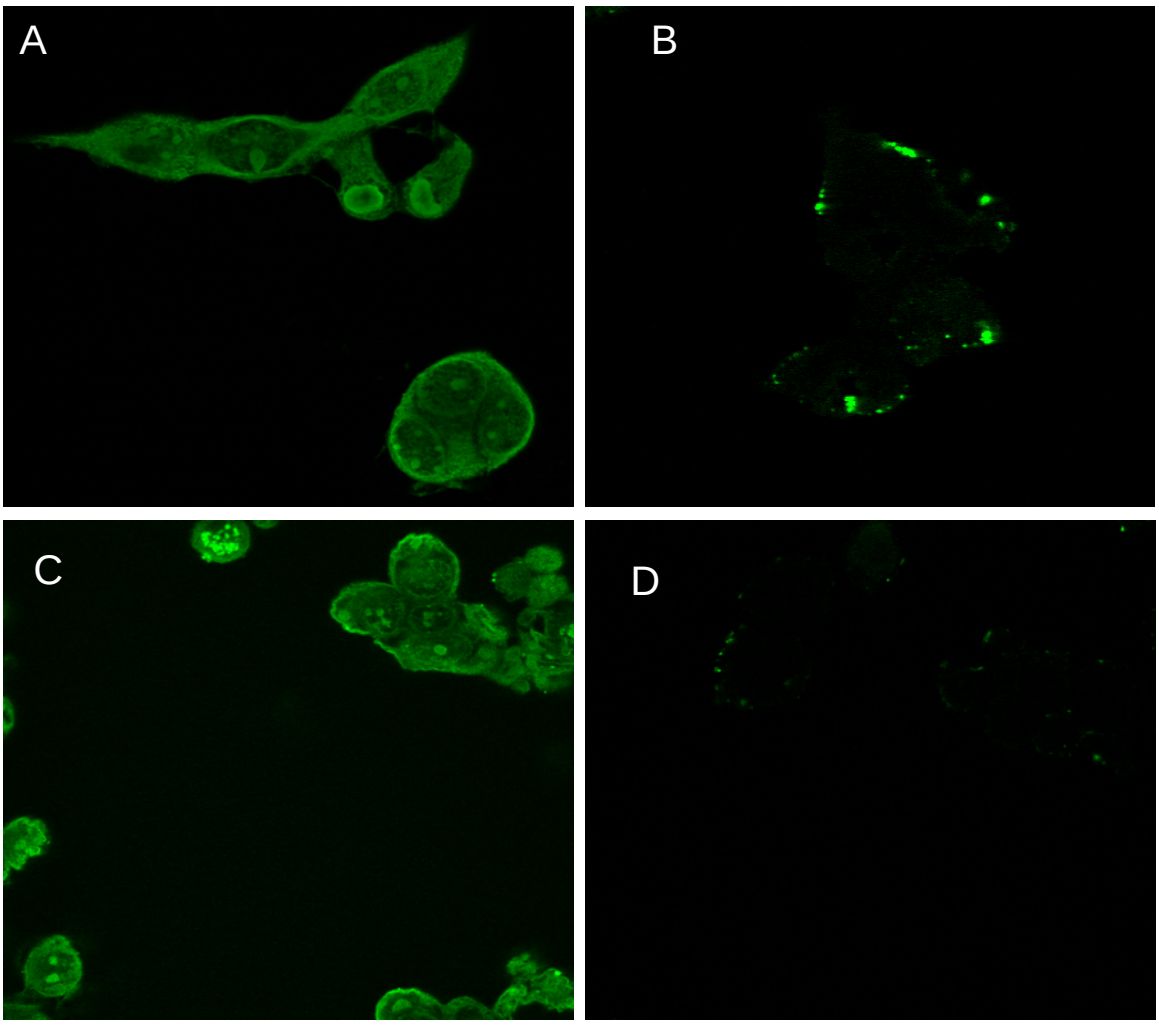

Figure 9. Staining results of T47D cells fixed before (panel A) and after (panel B) antibody staining. Panel C and panel D are MCF7 cells fixed before and after antibody staining and detection, respectively. These are single scan confocal images taken at the plane of best resolution.

Punctate cell membrane staining was best observed using post fixation (Figure 9b and Figure 9d). This observation conforms to expectations because somatostain is a membrane-bound protein (30, 39) and the antibody used in this experiment is designed to bind to the extracellular domain of the protein. Athough, punctate membrane staining was observed on the cells that were fixed after the antibody and Protein A-FITC application (Figure 9b and 9d), too many cells were lost from the

coverslips for this to be a routine procedure. From the results presented above for both T47D and MCF7 cells it was determined that fixation before antibody staining and detection was most useful.

Once the staining protocol was in place, we examined octreoate's effect on somatostatin staining at a cellular level in tissue culture. This experiment was conducted using T47D cells grown on glass coverslips.

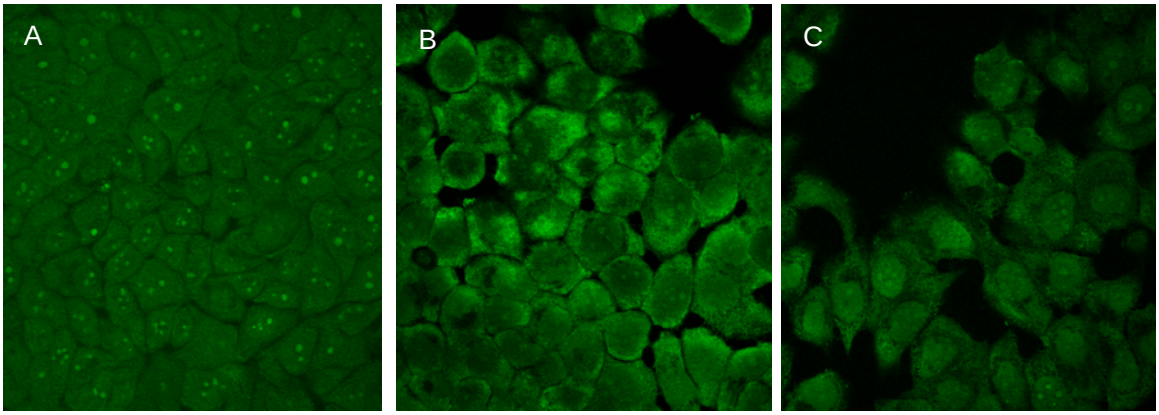

Figure 10. Octreoate's effect on somatostatin 2 receptor staining of T47D cells. The image in panel A is cells that were treated with octreoate before the anti-SSTr2 antibody; cells shown in panel B were treated with octreoate at the same time as the anti-SSTr2 antibody, and the image in panel C is cells that were treated with octreoate after the incubation with the anti-SSTr2 antibody. These are single scan confocal images taken at the plane of best resolution.

These images show that octreoate has a very high affinity for the SST2 receptors, actually replacing anti-somatostatin receptor 2 binding (Figure 10a) or out competing the somatostatin antibody at the receptor site (Figure 10b and 10c). This is shown by a much lower intensity staining compared to the images in Figure 9.

Immunohistochemical
Staining of Tumor Tissue

Having demonstrated positive SSTr2 staining in the tumor cell lines, the next step was to stain for the SST2 receptors in tumor tissue. This experiment could help to answer the question of whether our targeted PDT is affecting the tumor cells, the tumor vasculature or both. NCI H69 is a cell line that is known to express SST2 membrane receptors and was tested first.

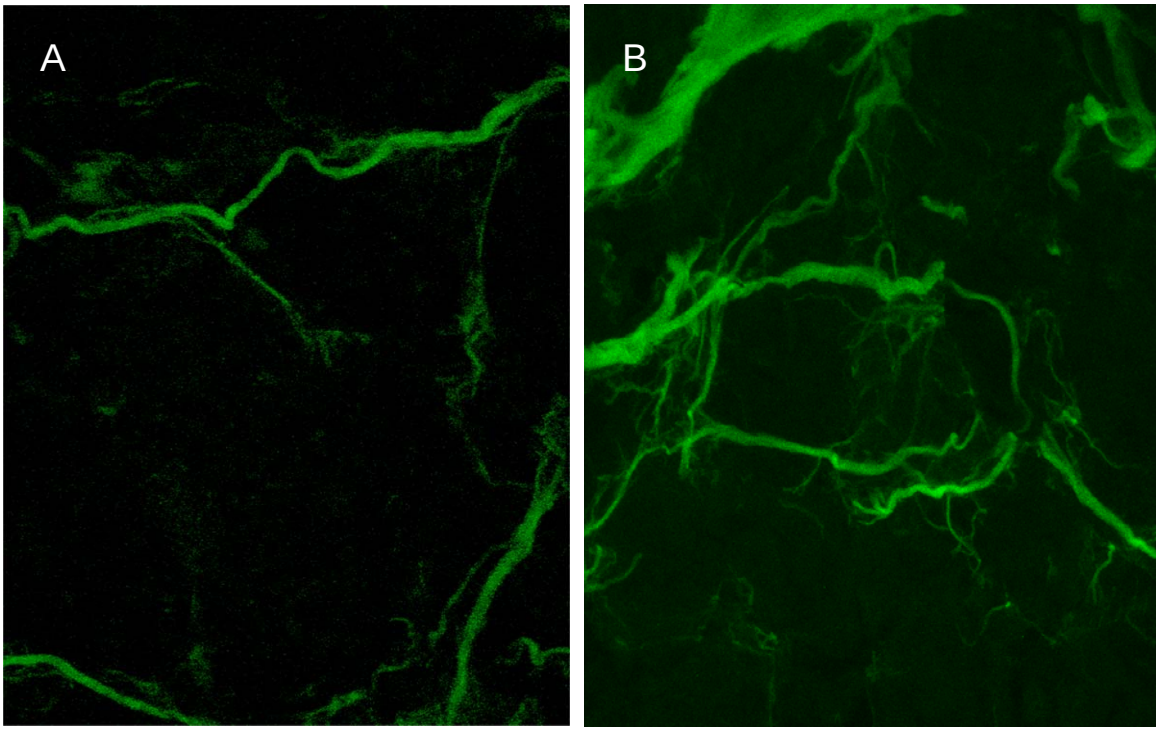

Figure 11. Results of NCI H69 tissue staining. Panel A depicts NCI H69 tumor tissue that was flash frozen and sectioned into 10 µm sections and stained for somatostatin 2 receptors. The anti-SSTr2 antibody was detected using Protein A-FITC. Panel B depicts NCI H69 tumor tissue that was flash frozen and sectioned into 10 µm sections and stained for vWF. The anti-vWF antibody was detected using Protein A-FITC. These images are each a reconstructed stack of confocal images.

The stained structures in the image shown in Figure 11, panel A resemble the pattern of tumor vessels. It is also noteworthy to mention how much more prominently the

vessels are stained versus the NCI H69 cells. To confirm that vessels were being stained, NCI H69 tumor tissue was also stained for vWF, a glycoprotein produced in the endothelium and a well recognized endothelial cell marker. The staining pattern in Figure 11, panel B is similar to that seen in Figure 11 panel A. To further convince observers that tumor vasculature was being stained in both cases, NCI H69 tumor tissue was double stained using both primary antibodies.

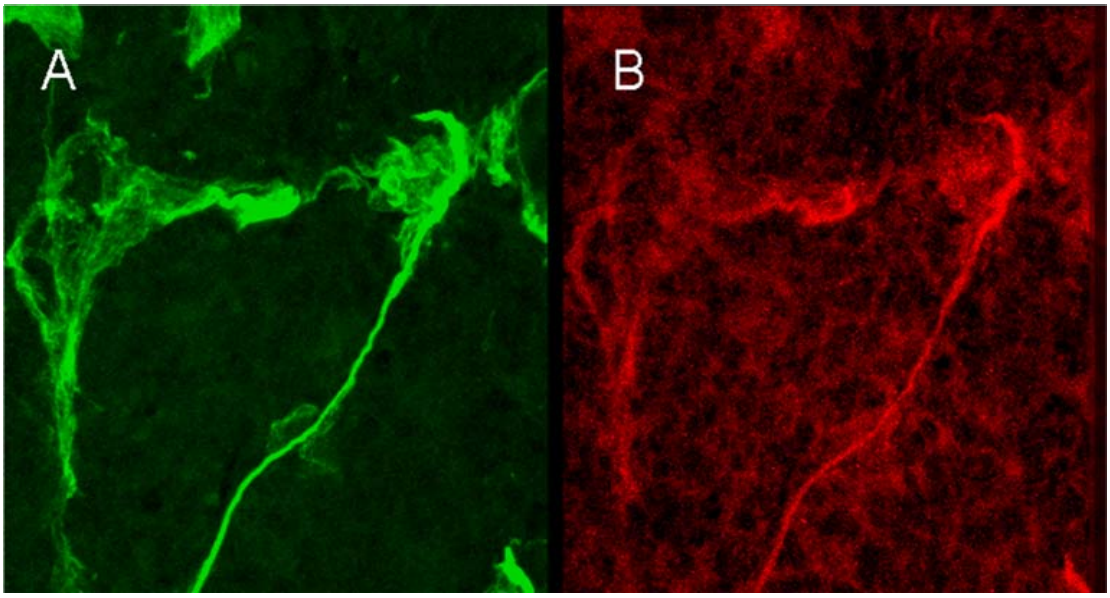

Figure 12. NCI H69 tumor tissue was flash frozen and sectioned into 10 µm sections and stained for vWF (panel A) and somatostatin receptor 2 (panel B). The anti-SSTr2 antibody was detected using Protein A-568 and the anti-vWF antibody was detected using Protein A-FITC. These images are reconstructed stacks of confocal images taken simultaneously through separate laser channels.

The same staining patterns presented in both panels of Figure 12 confirm that the tumor vasculature is being stained with anti-SSTr2 antibody.

The same staining procedures were conducted on a somatostatin receptor 2 negative cell line, A549. A549 tumor tissue was first stained for SSTr2.

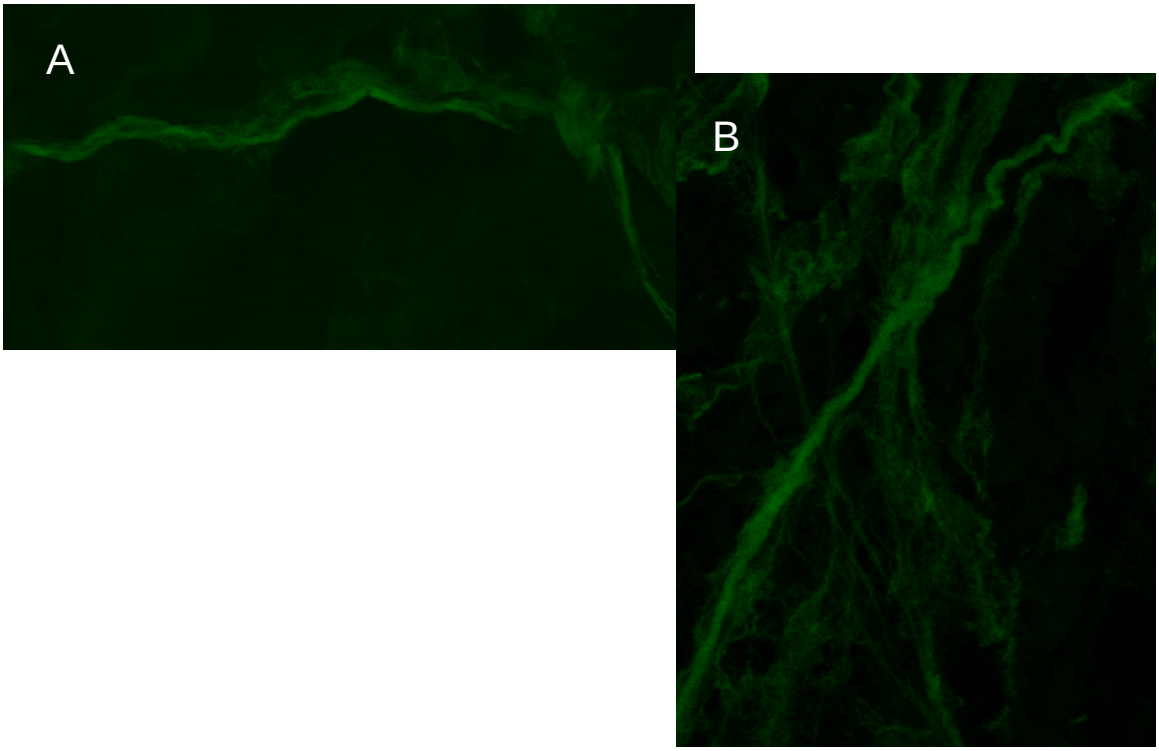

Figure 13. Results of A549 tissue staining. Panel A shows A549 tumor tissue that was flash frozen, sectioned into 10 μm sections and stained for SSTr2. The primary antibody was detected using Protein A-FITC. Panel B shows A549 tumor tissue that was flash frozen, sectioned into 10 μm sections and stained for vWF. The anti-vWF antibody was detected using Protein A-FITC. These images are each a reconstructed stack of confocal images.

Even though this cancer cell line is SSTr2 negative, the staining pattern is similar to that expected for tumor vessels (Figure 13a). In addition, the pattern is similar to that seen in Figure 11. Again, to confirm that vessels were being stained, A549 tumor tissue was stained for vWF. The staining pattern in Figure 13, panel B visualizes the tumor vessels. The vWF staining pattern in Figure 13, panel B is similar to the SSTr2 staining pattern of Figure 13, panel A. To further prove vessel staining for SSTr2, A549 tumor tissue was double stained using both anti-SSTr2 and anti-vWF primary antibodies.

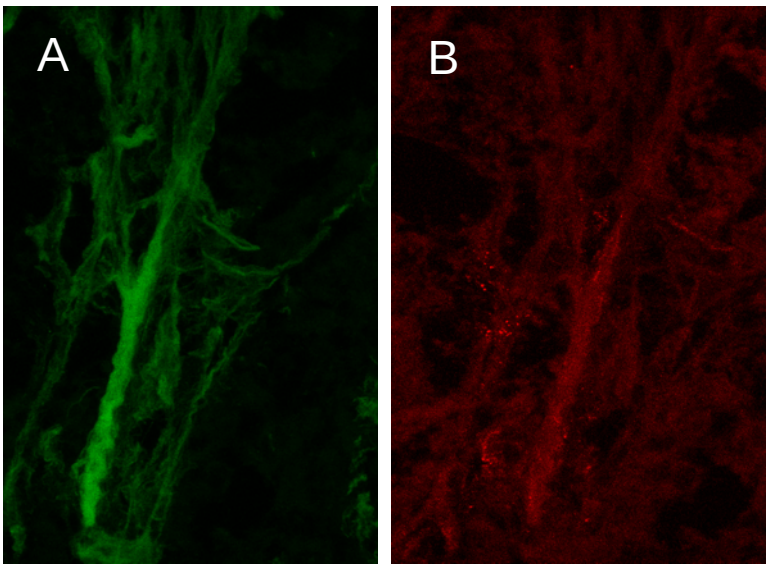

Figure 14. A549 tumor tissue was flash frozen and sectioned into 10 µm sections and stained for vWF (panel A) and somatostatin receptor 2 (panel B). The SSTr2 antibody was detected using Protein A-568 and the vWF antibody was detected using Protein A-FITC. These images are reconstructed stack of confocal images taken simultaneously using separate laser channels for each fluor.

From the results of staining A549 tumor tissue, the tumor vasculature of even SSTr2 negative cell lines can express somatostatin 2 receptors (Figure 13a and Figure 14b). This is significant because it could allow SSTr2 negative tumors to be effectively treated using our octreoate targeted PDT sensitizer. These results also provide insight as to how our targeted PDT works, effecting not only cancer cells, but also the tumor vasculature. Further experiments were done to confirm or reject this hypothesis.

Cellular Binding/Uptake of Octreoate Experiments

To answer the question of whether the targeted PDT photosensitizer was getting taken up by the tumor vasculature we needed a "tagged" octreoate. Octreoate was conjugated to biotin. In the primary reaction, octreoate conjugated to biotin

would bind to the somatostatin receptors. The detection method took advantage of the high binding affinity that biotin and avidin have for each other. NeutrAvidin conjugated to a Texas Red fluor was used in these experiments to visualize the biotinylated octreoate.

Octreoate Conjugation

As stated previously, octreoate was conjugated to biotin using EZ-link Amine-PEG3-Biotin (Pierce) following the manufacture's instructions. At the end of the conjugation process, the sample was purified using a Bio-Gel P-GDG desalting column. The fractions collected from the column were tested to demonstrate the presence of the biotinylated product. To do this an Immuno4 96-well plate was used. A small portion of each collection tube was added to one well. Detection utilized streptavidin conjugated to an Alexa Fluor 488 (Invitrogen). The fluorescence of the plate was checked on a Kodak scanner using filters appropriate for a 488 fluor.

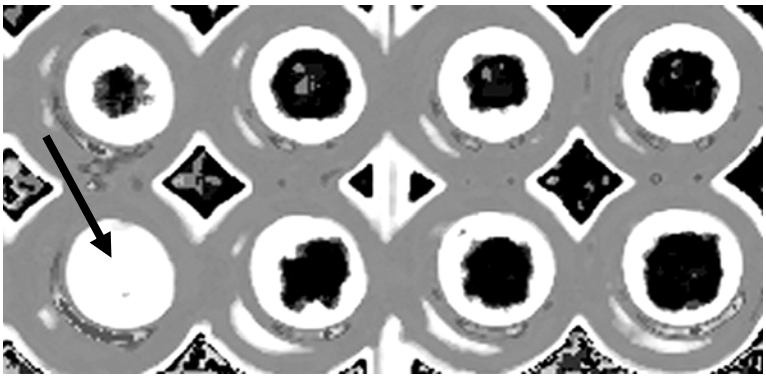

Figure 15. 96-well Immunon4 plate used to confirm the success of octreoate's conjugation to biotin. Fluorescence of the samples in each of the wells was read using a Kodak 2000 MM scanner equipped with a 448-500 nm bandpass excitation filter and a 535 emission filter. The arrow indicates a well containing a positive result for biotinylated octreoate.

If the well contained successfully biotinylated material the sample would bind to the well and the fluorescent streptavidin would bind sample in that well. The bound streptavidin would be detected by the scanner. Figure 15 shows an example positive well (bright well with the arrow) and several negative wells (wells that are dark and non-fluorescent) from the scan. Light scattering was evident around the edges of the negative wells, a normal effect from the scanner.

Presence of the biotinylated peptide was confirmed by reading the samples collected from the desalting column on a spectrophotometer at the $\lambda = 214$ absorption for peptide bonds. Based on the $\lambda = 214$ reading the fractions eluded from the desalting column were divided into three pooled samples (Table 1).

Table 1. $\lambda = 214$ reading boundaries. The sample's reading must fall within these boundaries to qualify for a sample designation. These readings were compared with control readings: MES coupling buffer has a $\lambda = 214$ of 1.17 and water has a $\lambda = 214$ reading of 0.01.

Sample	Low Spec Reading	High Spec Reading
Sample 1	1.47	1.48
Sample 2	1.02	1.46
Sample 3	0.08	0.66

Sample 1 had the highest $\lambda = 214$ readings compared to the positive control $\lambda = 214$ reading of MES coupling buffer so these collection samples were pooled as a positive conjugation result. Sample 1 (positive for biotin in the plate assay and showing peptide bond absorption at $\lambda = 214$) underwent further purification, was lyophilized

and reconstituted in 2.0 ml of water (a final concentration of 5 mg/ ml) for experimental use.

Cell Staining
Using Biotinylated Octreoate

Experiments, to see if octreoate was taken up by tumor cells and the cells of the tumor vasculature, were initiated on cells grown on glass coverslips in tissue culture. The cells were incubated with the biotinylated octreoate and the detection utilized NeutrAvidin- Texas Red.

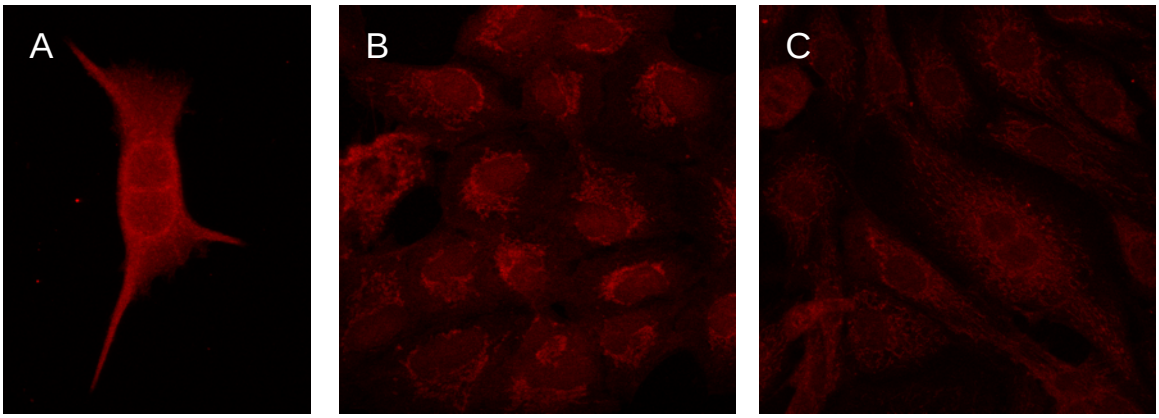

Figure 16. Tumor cells grown on coverslips and stained for somatostatin 2 repectors using biotinylated octreoate. The biotinylated octreoate is detected using NeutrAvidin-Texas Red. The cell lines are as follows: panel A shows T47D cells, panel B is A549 cells and panel C is bovine aortic endothelial (BAE) cells. Each of these images is a reconstructed stack of confocal images.

The structural similarities between the cells are apparent by observation. Each cell line exhibits strong peri-nuclear punctate staining. Overall staining was most intense for the SSTr2- positive T47D cell line (Figure 16a). In particular, T47D cells exhibited a more defined cellular membrane staining than either A549 (Figure 16b) or BAE (Figure 16c) cells.

Since tumor vascular endothelium exists in a milieu containing proangiogenic factors, the next experiment examined how endothelial cell growth factors might affect the SSTr2 staining of BAE cells. BAE cells were grown on glass coverslips and subjected to a variety of different growth conditions. The growth factors used were 10 ng/ml bFGF, 40 ng/ml VEGF, medium conditioned by proliferating A549 tumor cells and complete endothelial cell medium absent of any added growth factors. Somatostatin 2 receptors were stained using biotinylated octreoate and detected using NeutrAvidin- Texas Red.

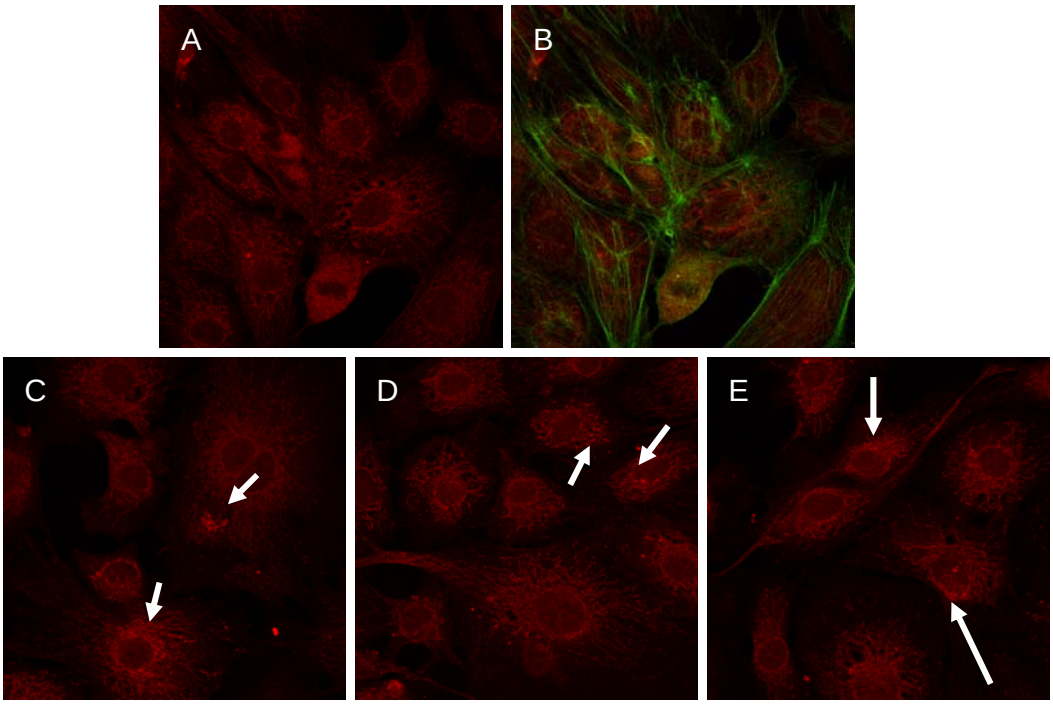

Figure 17. BAE cells grown on glass coverslips in medium containing different growth factors. Panel A shows cells in medium not containing any added growth factors and panel B shows the same cells as in panel A with an Alexa Fluor 488 Phalloidin counterstain. Panel C shows cells grown with added bFGF in the medium; panel D shows cells grown with added VEGF in the medium; and panel E shows cells grown with tumor conditioned medium. White arrows in this figure point out areas of high intensity staining indicating increased SSTr2 production. Each of these images is a reconstructed stack of confocal images. Images in panels A and B were taken simultaneously using separate laser channels for each fluor.

The bFGF and VEGF did affect the endothelial cells. Not only did the cells grow more rapidly in culture, exhibited by an increased number of mitotic figures and a shorter time of growth to reach confluency, but the cells exhibited more perinuclear staining (white arrows in Figure 17c and Figure 17d). The endothelial cells also grew more rapidly in tumor conditioned medium, although this effect was less than for the isolated growth factors. These cells also showed more perinuclear staining (Figure 17e). The cytoskeletal counterstain was done to examine if octreoate was localizing with actin components of the cell cytoskeleton (Figure 17b). In all conditions, there was weak cell membrane staining.

Tissue Staining
Using Biotinylated Octreoate

To observe octreoate binding/uptake into endothelial cells of the tumor vasculature, tumor tissue sections were stained using the biotinylated octreoate. NCI H69 and A549 lung tumor tissue was used in this experiment.

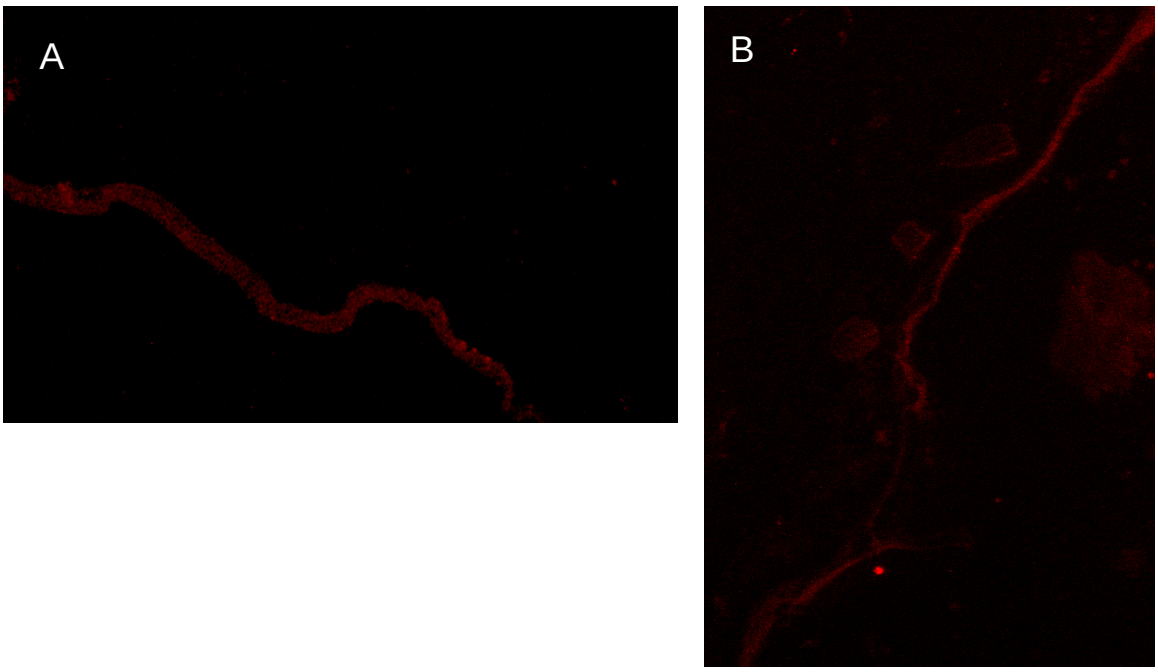

Figure 18. Lung tumor tissue was cut into 10 μm sections and stained for somatostatin 2 receptors using biotinylated octreoate detected with NeutrAvidin-Texas Red. Panel A is a NCI H69 tissue section. Panel B is an A549 tissue section. Images in each individual panel are a reconstructed stack of confocal images.

The staining patterns depicted in both panels of Figure 18 mimic the staining patterns of previous tissue sections of confirmed tumor vessels. The staining pattern observed in both panels of Figure 18 also imitates the pattern expected of vessels. The tumor vasculature staining was confirmed by double staining lung tumor sections in two separate procedures. The first stained for somatostatin receptors using biotinylated octreoate and an Alexa Fluor 488 Phalloidin counterstain (Figure 19a and 19b), and the second stained for somatostatin 2 receptors using biotinylated octreoate and a primary ant-vWF antibody (Figure 19c and 19d).

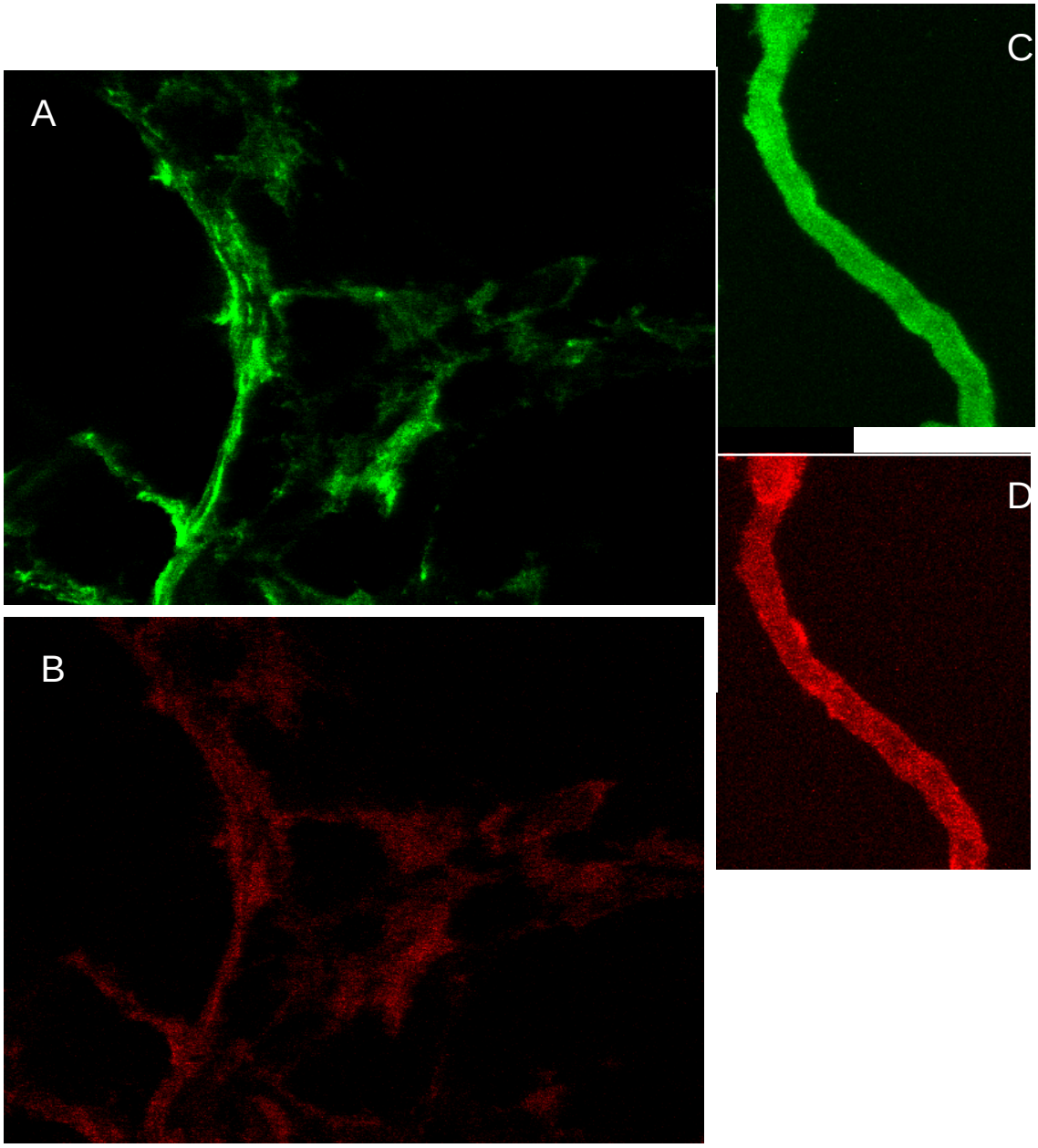

Figure 19. Panel A and panel B depict A549 tissue samples cut into 10 µm sections and stained for SSTr2 using biotinylated octreoate detected using NeutrAvidin- Texas Red (panel B) followed by a counterstain using Alexa Fluor 488 Phalloidin (panel A) to detect polymerized actin. The inset panel C and panel D depict a putative vessel in a NCI H69 tissue section double stained using biotinylated octreoate detected using NeutrAvidin- Texas Red to stain for SSTr2 (panel D) and for vWF using anti-vWF primary antibody detected using Protein A-FITC (panel C). Images in each individual panel are a reconstructed stack of confocal images. Images of panels A and B as well as panels C and D were taken simultaneously through separate laser channels for each fluor.

The counterstain using Phalloidin Alexa Fluor 488 (Figure 19a) shows how little polymerized actin the tumor cells have, while the endothelial cells of the proposed tumor vasculature exhibit a much more prominent staining pattern. The actin staining pattern of the counterstain matches the staining pattern of the conjugated octreoate staining for SSTr2 (Figure 19b). The double staining images of NCI H69 tumor tissue is not shown but results were as expected in that the small round cells do not have a lot of polymerized actin, and therefore there was weak counterstain signal. The inset images depict NCI H69 tumor tissue double stained for vWF (Figure 19c) and for SSTr2 using biotinylated octreoate (Figure 19d). The membrane staining SSTr2 pattern matches the vWF staining pattern, and these images show that the biotinylated octreoate is binding to receptors on endothelial cells of this tumor vessel.

CHAPTER 4

DISCUSSION

Photodynamic therapy is a cancer treatment which uses the combination of a photosensitizing drug and light to selectively kill cancer cells. PDT promises to be important in the future of cancer treatment in part because the PDT drug can selectively accumulate in the tumor microenvironment, or can be made to target the cancer cells. Thus, the treatment only affects the cancer and not the entire body, unlike many other cancer treatment options that are available. Studies have shown that PDT not only acts on cancer cells by producing cytotoxic singlet oxygen, but also activates the immune system, and can destroy tumor vasculature depriving the tumor cells of essential oxygen and nutrients.

Angiogenesis is a physiological process involving the growth of new blood vessels from pre-existing ones (51). Angiogenesis is a normal, but highly regulated, process in growth and development occurring most frequently during wound healing, embryonic development, and in the female reproductive cycle (53). The role of angiogenesis in cancer development is well accepted. If a tumor mass is to grow beyond a few millimeters in size the "angiogenic switch" must occur (53). Angiogenesis is initiated from the production and release of angiogenic growth factors from cancer cells (52). Examples of angiogenic growth factors are VEGF and bFGF which are used in this study. Upon stimulation from these growth factors endothelial cells become activated. The activated endothelial cells break down the

underlying basement membrane, proliferate and migrate. The migrating cells attach to integrin adhesion molecules and sprout new blood vessels (60).

Tumor vasculature represents an important target for cancer therapy and second generation photosensitizers are taking advantage of the tumor cell dependence on a functional blood supply for continued growth (59). Photosensitizers such as Tookad® are being used to treat cancer by damaging the tumor vasculature. In the clinic, the drug is injected intravenously and, immediately following this, the tumor area is illuminated. The drug is still contained within the vessels and the generation of singlet oxygen causes endothelial cell killing (15). The destroyed tumor vasculature can no longer supply the tumor with oxygen and nutrients and the tumor cells die of starvation.

Several tumor cell lines used in the lab are engineered to express the luciferase gene. As the cells grow in mice, tumors can be monitored by injecting luciferin and visualizing the resultant bioluminescence using *in vivo* imaging. The luciferase activates a chemical reaction of the luciferin producing light. Tumors were monitored in this manner before and after PDT treatment and it was observed that there was more light produced before treatment than after. This observation led to two possible conclusions: a) cancer cells were destroyed or b) the luciferin was not circulating to the tumor due to damaged tumor vasculature. The experiments carried out during the current study focused on determining if our novel PDT sensitizer could combine the benefits of not only targeting the cancer cells but also destroying the tumor vasculature.

The first set of experiments utilized *in vivo* imaging, after intravenously injected FITC dextran, to examine the integrity of the tumor vasculature before and after PDT treatment. Octreoate was used to block somatostatin 2 receptors and prevent our PDT drug from binding. Without the octreoate block, the images show a remarkable difference in the amount of fluorescence before treatment (Figure 6a) and after treatment (Figure 6b) image. In contrast, when octreoate was used to block SSTr2 the amount of fluorescence detected was similar (Figure 6c and d). Without the octreoate block the lack of fluorescence after treatment indicated that the FITC dextran was not able to circulate to the tumor because the vasculature had been damaged. The effectiveness of PDT treatment was confirmed by measuring and evaluating tumor growth following treatment in mice. As observed in Figure 7, mice that received no treatment or an octreoate injection followed by PDT treatment experienced rapid and extensive growth of the tumor. Mice that received PDT treatment exhibited initial reduction in size of the tumor followed by much slower tumor growth. These experiments show the efficacy of the targeting moiety of the PDT drug. When unable to bind to somatostatin 2 receptors the drug is ineffective, and treatment using PDT is not successful. Similar amounts of FITC dextran delivery in the tumor before and after treatment in the octreoate treated mice indicated that the vasculature was not damaged during treatment; furthermore, tumor growth rates demonstrated that PDT treatment was not effective after octreoate block.

The next set of experiments focused on using tumor cells in culture. SSTr2-positive and SSTr2- negative cell lines were stained using an anti-SSTr2 antibody to

demonstrate the presence of receptors on the tumor cells. SSTr2- positive breast cancer cell line, T47D, exhibited punctate membrane staining in addition to prominent nucleolar staining. Punctate membrane staining can be seen when staining for many tumor cell receptors because receptors are not uniformly distributed on the surface. Staining procedures may also induce aggregation of receptors. Overall staining was much weaker with the introduction of octreoate, demonstrating the cell line does express the SST2 receptors on its cell surface and, therefore, can be targeted by our PDT drug.

After observing the positive tumor cell staining, the next step was to examine tumor tissue. By studying tumor tissue, both tumor cells and tumor vasculature could be examined. Images of tumor tissue showed positive SSTr2 staining patterns of the tumor vasculature in both SSTr2- positive NCI H69 tumor sections (Figure 11a) and SSTr2- negative A549 tumor sections (Figure 13a). The vascular staining of the NCI H69 tissue section was much more prominent than the staining of the tumor cells. It has been reported that SSTr2 expression is upregulated several-fold in vasculature located within 2 cm of a tumor (56). The positive SSTr2 staining of the A549 tumor vasculature could expand the use of our targeted PDT sensitizer because treatment would not be limited to tumors whose cells overexpress SSTr2. If the endothelial cells comprising the tumor vasculature are SSTr2 positive and can bind the drug they will be susceptible to PDT killing. The strong SSTr2 staining of the tumor vasculature could indicate an important mechanism through which our PDT protocol treats cancer.

In the double staining experiments of tumor tissue, it would have been beneficial to have an additional negative control in which each primary antibody was used individually with the sequential application of both the Protein A-FTIC and the Protein A-568. This would examine the possibility that in the double staining experiments, using two primary antibodies, each detected using a Protein A, that Protein A-FITC and Protein A-568 were detecting the same antibody.

Other studies have determined that angiogenic blood vessels of tumors do express SSTr2 at the gene level but it was initially unclear if the genes were translated into proteins (54). More recently, it was reported that endothelial cells in proliferating human blood vessels express SSTr2 (55, 58). Since angiogenesis is occurring during tumor development, the tumor vessels will express SSTr2 and will be targeted by our PDT agent. Normal endothelial cells would not be affected by SSTr2 targeted PDT because they are normally quiescent, dividing only once every 2–5 years (61).

The next question was if our targeted PDT drug was getting internalized into the endothelial cells. For this experiment the somatostatin analog, octreoate, was conjugated to biotin. The biotin's only function was in detection; the detection method in these experiments used NeutrAvidin conjugated to a Texas Red fluor. Cell staining patterns from this experiment show organized punctuate membrane staining from T47D cells (Figure 16a). However, the staining patterns of the endothelial cells used in this experiment more closely resemble the intricate peri-nuclear staining shown in the A549 cells (Figure 16c and b). This could be due to the fact that

proliferation in cell culture may not be accompanied by surface expression of SSTr2. Based on the literature (40), A549 cells were used as the SSTr2- negative cell line our experiments. However, the staining pattern obtained in the results of this experiment would seem to indicate that A549 cells are producing the somatostatin 2 receptor. These contradicting observations are resolved with the observation of definite peri-nuclear staining but no membrane staining concluding that the A549 tumor cell line does produce SSTr2 but does not express these receptors on the cell surface.

The next experiment was designed to test aspects of the tumor microenvironment to examine if membrane SSTr2 staining could be induced in BAE cells. Endothelial cell growth factors were added to the media and the cells were grown in culture and stained the using biotinylated octreoate and NeutrAvidin Texas Red. In culture, VEGF and bFGF as well as A549 conditioned media caused the BAE cells to grow approximately twice as fast. The images obtained from this experiment showed exaggerated peri-nuclear staining (Figure 17) when compared to cells grown in normal medium conditions. Increased peri-nuclear staining signifies increased production of SSTr2. Lack of clear membrane staining, however, indicates that the growth factors used do not stimulate membrane localization of endothelial SSTr2 production. Although VEGF and bFGF were obvious choices to begin experimentation (33), others of the over 20 documented endothelial cell growth factors likely lead to SSTr2 membrane localization. If the study were repeated, appropriate choices might be transforming growth factor- alpha (TGF-alpha), pleiotrophin (PTN) or interleukin-8 (IL-8). Conditioned medium from the A549 cell

line was chosen because these cells do not express somatostatin 2 receptors on their cell surface simplifying analysis of results. If conditioned medium from a different tumor cell line was used it could easily lead to different results. Should the study be repeated, conditioned medium would also be taken from a cell line that does express SSTr2 on its membrane, such as T47D.

Images obtained from staining for somatostatin 2 receptors, using the conjugated octreoate in NCI H69 and A549 (Figure 18) tumor tissue sections, show positive SSTr2 staining. The staining pattern mimics that of tumor vasculature indicating the octreoate was bound by the endothelial cells. The vessels exhibit stronger staining patterns than the tumor cells. A study completed by Watson *et.al.* using a radiolabelled somatostatin analog also showed vascular uptake and indicated that this would enable tumor imaging of SSTr2- negative tumors (55). This provides another use for targeting the SSTr2 on tumor vasculature.

Limitations of This Study

In the course of this study we found a limitation involving confocal microscope equipment. In the experiment involving using a dye to detect octreoate and its uptake within the cancer cells, the dye desired for use was the Licor CW 800 because it is the NIR imaging fluor that is going to be used in future whole animal studies. However, this dye could not be used because, although MSU has a confocal microscope that could excite the Licor CW 800 dye, MSU does not have a confocal microscope with detectors sensitive enough in the NIR region of the spectrum to

detect the emission of this dye. Therefore, Texas Red was used as the fluor in the uptake experiments, instead.

CHAPTER 5

CONCLUSIONS AND FUTURE DIRECTIONS

Vascular targeted PDT sensitizers represent one of the newest generation of photosensitizers (62). However, the preference of vascular versus cellular targeting is highly dependent upon the location of the photosensitizer at the time of light illumination (63). In most cases treatment relies on strategic drug – light interval timing and not on strategic targeting using drug moieties. Based on experimental data it is evident the endothelial cells comprising the tumor vasculature express SSTr2. Our novel PDT drug is unique in not only targeting tumor cells but targeting the tumor vasculature as well. Targeting, treating and shutting down the tumor vasculature are important mechanisms in the way our PDT protocol treats cancer.

PDT has the potential to decrease morbidity effects from treatment and improve quality of life for patients with many health conditions and diseases. It also has the potential to improve health economics (6). Future improvements involve using the immune system activating properties of PDT in combination with other immunotherapy protocols to control tumor growth on a more long term basis (2). As new, better, photosensitizers are developed, pharmaceutical companies will look to expand the conditions and diseases PDT can treat. This involves improved drug delivery systems for better tumor targeting, such as, using liposomes, ligand-based targeting with, for example, insuln, and using growth factors or adenoviruses (4).

PDT could also be improved by using new light sources to increase penetration into the tissue.

Future directions for our PDT study will involve larger animal (canine and rabbit) testing to accurately measure the maximal depth of tissue penetration that is possible using 2PA PDT. Increased depth of penetration will expand the potential uses for 2PA PDT because it would allow treatment of tumors that are located deep within the body and/or are not accessible by minimally invasive surgery.

REFERENCES CITED

1. Krammer, Barbara. Vascular effects of photodynamic therapy. *Anticancer Research* 21: 4271-4278, 2001.

2. Dougherty, Thomas, Charles J. Gomer, Barbara W. Henderson, Giulio Jori, David Kessel, Mladen Korbelik, Johan Moan, and Qiun Peng. *Journal of the National Cancer Institute* 90(12): 889-905, 1998.

3. Usada, Jitsuo, Harubumi Kato, Tetsuya Okunaka, Kinya Furukawa, Hidemitsu Tsutsui, Kimito Yamada, Yasuhito Suga, Hidetoshi Honda, Yoshitaka Nagatsuka, Tatsuo Ohira, Masahiro Tsuboi, and Takashi Hirano. Photodynamic therapy (PDT) for lung cancers. *Journal of Thoracic Oncology* 1(5): 489-493, 2006.

4. Wiedmann, Marcus, and Karel Caca. General principles of photodynamic therapy (PDT) and gastrointestinal applications. *Current Pharmaceutical Biotechnology* 5: 397-408, 2004.

5. Triesscheijn, Martijn, Paul Baas, Jan H.M. Schellens, and Fiona A. Stewart. Photodynamic therapy in oncology. *The Oncologist* 11: 1034-1044, 2006.

6. Brown, Stanley B, Elizabeth A Brown, and Ian Walker. The present and future role of photodynamic therapy in cancer treatment. *The Lancet* 5: 497-508, 2004.

7. Photodynamic Therapy. April 2, 1997. Smith Group Website. June 2008. http://chemgroups.ucdavis.edu/~smith/PDT_Reserach/PDT.html.

8. Ochsner, M. Photophysical and photobiological processes in the photodynamic therapy of tumors. *Journal of Photochemistry and Photobiology* 39: 1-18, 1997.

9. Josefsen, LB, and RW Boyle. Photodynamic therapy: novel third-generation photosensitizers one step closer? *British Journal of Pharmacology* 154: 1-3, 2008.

10. Hamblin, Michael R, and Tayyaba Hasan. Photodynamic therapy: a new antimicrobial approach to infectious disease? *Photochem. Photobiol. Sci.* 3: 436-450, 2004.

11. Korbelik, Mladen, Jinghai Sun, and Ivana Cecic. Photodynamic therapy-induced cell surface expression and release of heat shock proteins: relevance for tumor response. *Cancer Research* 65(3): 1018-1026, 2005.

12. Awan, M.A., and S.A. Tarin. Review of Photodynamic therapy. *Surgeon* 4(4): 231-236, 2006.

13. Kato, H., J. Usuda, T. Okunaka, K. Furukawa, H. Honda, N. Sakaniwa, Y. Suga, T. Hirata, K. Ohtani, T. Inoue, S. Maehara, M. Kubota, and K. Yamada. Basic and clinical research on photodynamic therapy at Tokyo Medical University Hospital. *Lasers in Surgery and Medicine* 38: 371-375, 2006.

14. Levy, Julia G. New photosensitizers for photodynamic therapy. Annual International Conference of the IEEE Engineering in Medicine and Biology Society 12(3): 1138-1139, 1990.

15. Woodhams, Josephine H., Alexander J. MacRobert, Marco Novelli, and Stephen G. Brown. Photodynamic therapy with WST09 (Tookad): quantitative studies in normal colon and transplanted tumours. *International Journal of Cancer* 118: 477-482, 2006.

16. Castano, Ana, Pawel Mroz, and Michael R. Hamblin. Photodynamic therapy and anti-tumor immunity. *Nature Reviews* 6: 535-545, 2006.

17. Korbelik, Mladen, Jinghai Sun, Ivana Cecic, and Katherine Serrano. Adjuvant treatment for complement activation increases the effectiveness of photodynamic therapy of solid tumors. *Photochem. Photobiol. Sci.* 3: 812-816, 2004.

18. Gollnick, Sandra O., Barbara Owczawczak, and Patricia Maier. Photodynamic therapy and anti-tumor immunity. *Lasers in Surgery and Medicine* 38: 509-515, 2006.

19. Canti, Gianfranco, Alessandra De Simone, and Mladen Korbelik. Photodynamic therapy and the immune system in experimental oncology. *Photochem. Photobiol. Sci.* 1: 79-80, 2002.

20. Kabingu, E, L Vaughan, B Owczarczak, KD Ramsey, and SO Gollnick. CD8+ T cell-mediated control of distant tumours following local photodynamic therapy is independent of CD4+ T cells and dependent on natural killer cells. *British Journal of Cancer* 96(12): 1839-1848, 2007.

21. Kousis, Philaretos C., Barbara W. Henderson, Patricia G. Maier, and Sandra O. Gollnick. Photodynamic therapy enhancement of antitumor immunity is regulated by neutrophils. *Cancer Research* 67(21): 10501-10510, 2007.

22. Mantovani, Alberto, Pedro Romero, A Karolina Palucka, and Francesco M Marincola. Tumour immunity: effector response to tumour and role of the microenvironment. *The Lancet* 371: 771-783, 2008.

23. Breast Cancer. December 12, 2007. National Cancer Institute. June 2008. http://www.cancer.gov.
Lung Cancer. December 12, 2007. National Cancer Institute. June 2008. http://www.cancer.gov.

24. Breast Cancer. September 26, 2007. MayoClinic. June 2008. http://www.mayoclinic.com/healthbreast-cancer/.
Lung Cancer. November 10, 2007. MayoClinic. June 2008. http://www.mayoclinic.com/healthlung-cancer/.

25. Lung Cancer. June 6, 2008. Centers for Disease Control and Prevention. June 2008. http://www.cdc.gov/cancer/lung/.

26. Ogawa, Kazuya, and Yoshiaki Kobuke. Recent advances in two-photon photodynamic therapy. *Anti-Cancer Agents in Medicinal Chemistry* 8: 269-279, 2008.

27. Arnbjerg, Jacob, Mette Johnsen, and Peter R. Ogilby. Two-photon photosensitized singlet oxygen production. *The Spectrum* 21(1): 20-27, 2008.

28. Spangler, C.W., J.R. Starkey, A. Rebane, F. Meng, A. Gong, M. Drobizhev. Synthesis, characterization and preclinical studies of two-photon-activated targeted PDT therapeutic triads. *Proc. Of SPIE* 6139: 6139OX-1-6139OX-10, 2006.

29. Spangler, Charles W. Overview of targeted two-photon PDT- image- driven PDT. 2006.

30. Chen, Longchuan, and Armen H. Tashjian, Jr. Identification of distinct signaling pathways for somatostatin receptors SSTR1 and SSTR2 as revealed by microphysiometry. *Cellular Signal.* 11(7): 499-505, 1999.

31. Rivera Juan A., Haydar Alteraihi, and Ujendra Kumar. Differential regulation of somatostatin receptors 1 and 2 mRNA and protein expression by tamoxifen and estradiol in breast cancer cells. *Journal of Carcinogenesis* 4(10): 1-10, 2005.

32. Froidevaux, Sylvie, Edith Hintermann, Michael Torok, Helmut R. Macke, Christoph Beglinger, and Alex N. Eberle. Differential regulation of somatostatin receptor type 2 (sst 2) expression in AR4-2J tumor cells implanted into mice during octreoate treatment. *Cancer Research* 59: 3652-3657, 1999.

33. Hussain, Sajjad, Mark Slevin, Mohammad A. Mesaek, Mohammad I. Choudhary, Abdul H. Elosta, Sabine Matou, Nessar Ahmed, David West, and John Gaffney. Cheiradone: a vascular endothelial cell growth factor receptor antagonist. *BMC Cell Biology* 9(7): 1-10, 2008.

34. Tulipano, Giovanni, Ralf Stumm, Manuela Pfeiffer, Hans-Jurgen Kreienkamp, Volker Hollt, and Stefan Schulz. Differential β-arrestin trafficking and endosomal sorting of somatostatin receptor subtypes. *The Journal of Biological Chemistry* 279(20): 21374-21382, 2004.

35. Li, Bing, Jian Yao, Kazuko Kaw, Yukiko Oyanagi-Tanaka, Mari Hoshiyama, Tetsuo Morioka, Fumitake Gejyo, Makoto Uchiyama, and Takashi Oite. Real-time observation of glomerular hemodynamic changes in diabetic rats: effects of insulin and ARB. *Kidney International* 66: 1939-1948, 2004.

36. IHC Washing Buffer. 2007. IHC World. 2006. http://www.ihcworld.com/_protocols/washing-buffers/pbs.htm.

37. Inai, Tetsuichiro, Michael Mancuso, Hiroya Hashizume, Fabienne Baffert, Amy Haskell, Peter Baluk, Dana D. Hu-Lowe, David R. Shalinsky, Gavin Thurstron, George D. Yancopoulos, and Donald M. McDonald. Inhibition of vascular endothelial growth factor (VEGF) signaling in cancer causes loss of endothelial fenestrations, regression of tumor vessels, and appearance of basement membrane ghosts *American Journal of Pathology* 165(1): 35-52, 2004.

38. Bernd, Antje S., Makoto Aihara, James D. Lindsey, and Robert N. Weinreb. Influence of molecular weight on intracameral dextran movement to the posterior segment of the mouse eye. *Investigative Ophthalmology and Visual Science* 45(2): 480-484, 2004.

39. Reubi, Jean Claude, Beatrice Waser, Jean-Claude Schaer, and Jean A. Laissue. Somatostatin receptor sst1 – sst5 expression in normal and neoplastic human tissues using receptor autoradiography with subtype-selective ligands. *European Journal of Nuclear Medicine* 28(7): 836-846, 2001.

40. Nayak, Tapan, Jeffrey Norenberg, Tamara Anderson, and Robert Atcher. A comparison of high-versus low-linear energy transfer somatostatin receptor targeted radionucleotide therapy *in vitro. Cancer Biotherapy and Radiopharmaceuticals* 20(1): 52-57.

41. Gitlin, Gerry, Edward A. Bayer, and Meir Wilchek. Studies on the biotin-binding sites of avidin and streptavidin. *Biochem. J.* 269: 527-530, 1990.

42. Avidin and NeutrAvidin™Biotin-Binding Proteins and Conjugates. April 2, 2002. Molecular Probes Product Information. July 2008. http://probes.invitrogen.com/handbook/.

43. Toth, B, R. Neuwland, S. Liehardt, N. Ditsch, K. Steinig, P. Stieber, A. Rank, P. Gohring, C.J. Thater, K. Friesek, and I. Bauerfeind. Circulating microparticles in breast cancer patients: a comparative analysis with established biomarkers. *Anticancer Research* 28(2A): 1107-1112, 2008.

44. Wong, J., W. Bennett, M.W. Ferguson, and D.A. McGrohther. Microscopic and histological examination of the mouse hindpaw digit and flexor tendon arrangement with 3D reconstruction. *Journal of Anatomy* 209(4): 533-545, 2006.

45. van den Boogert, Jolanda, Adraiaan B. Houtsmalller, Felix W.M. de Rooij, Ron W.F. de Brian, Peter D. Siersema, and Richard van Hillegersberg. Kinetics, localization, and mechanism of 5-aminoculinic acid-induced porphyrin accumulation in normal Barrett's-like rat esophagus. *Lasers in Surgery and Medicine* 24(1): 3-13, 1999.

46. Yang, M.Y., and J.R. Fortune. Vascular endothelial growth factor stimulates the primary to secondary follicle transition in bovine follicles *in vitro*. *Molecular Reproduction and Development* 74: 1095-1104, 2007.

47. Takayanagi, Shin-ichiro, Takashi Hiroyama, Satoshi Yamazaki, Tomoko Jakajima, Yohei Morita, Joichi Usai, Koji Eto, Tsutomu Motohashi, Kensuke Shiomi, Kazuko Keino-Masu, Masayuki Masu, Yuichi Oike, Shigeo Mori, Nobuaki Yoshida, Stsushi Iwama, and Hiromitsu Nakauchi. Genetic marking of hemotopoietic stem and endothelial cells: identification of the *Tmtsp* gene encoding a novel cell surface protein with the thrombospondin-1 domain. *Blood* 107(11): 4317-4325, 2006.

48. Arbiser, Jack L., Helena Larsson, Lena Claesson-Welsh, Xianhe Bai, Kenneth LaMontagne, Sharon W. Weiss, Shai Soker, Evelyn Flynn, and Lewrence F. Brown. Overexpression of VEGF 121 in immortalized endothelial cells causes conversion to slowly growing angiosarcoma and high level expression of the VEGF receptors VEGFR-1 and VEGFR-2 *in vivo*. *American Journal of Pathology* 156(4): 1469-1476, 2000.

49. Xu, Ren-He, Ruthann M. Peck, Dong S. Li, Xuezhu Feng, Tenneille Ludwig, and James A. Thomson. Basic FGF and suppression of BMP signaling sustain undifferentiated proliferation of human ES cells. *Nature Methods* 2(3): 185-190, 2005.

50. Hermant, Bastien, Agnes Desroches-Castan, Marie-Laure Dubessay, Marie-Helene Prandini, Philippe Huber, and Danial Vittet. Development of a one-step embryonic stem cell-based assay for the screening of sprouting angiogenesis. *BMC Biotechnology* 7(20): 1-9, 2007.

51. Folkman, Judah, Angiogenesis. *Annual Reviews in Medicine* 57: 1-18, 2006.

52. Weinberg, Robert A. The Biology of Cancer. New York: Garland Science, Taylor & Francis Group, LLC, 2007.

53. de la Torre, N. Garcia, J. A. H. Wass, and H. E. Turner. Antiangiogenic effects of somatostatin analogs. *Clinical Endocrinology* 57: 425-441, 2002.

54. Woltering, Eugene A. Development of targeted somatostatin-based antiangiogenic therapy: a review and future perspectives. *Cancer Biotherapy and Radiopharmaceuticals* 18(4): 601-609, 2003.

55. Watson, JC, DA Balster, BM Gebhardt, TM O'Dorislo, MS O'Dorislo, GD Espenan, GJ Drouant, and EA Woltering. Growing vascular endothelial cells express somatostatin subtype 2 receptors. *British Journal of Cancer* 85(2): 266-272, 2001.

56. Denzler, Barbara, and Jean C. Reubi. Expression of somatostatin receptors in peritumoral veins of human tumors. *Cancer* 85(1): 188-198, 1999.

57. McDonald, Donald M., and Alexander J.E. Foss. Endothelial cells of tumor vessels: abnormal but not absent. *Cancer and Metastasis Reviews* 19: 109-120, 2000.

58. Adams, RL, IP Adams, and SL Atkin. Expression of somatostatin receptors in proliferating and quiescent endothelial cells. *Endocrine Abstracts* 5: 146, 2003.

59. He, Chong, Priyanka Agharkar, and Bin Chen. Intravital microscope analysis of vascular perfusion and macromolecule extravasation after photodynamic vascular targeted therapy. *Pharmaceutical Research* 2008.

60. Abels, Christoph. Targeting of the vascular system of solid tumours by photodynamic therapy (PDT). *Photochem. and Photobiol. Sci.* 3: 765-771, 2004.

61. Adams, RL, IP Adams, SW Lindow, W Zhong, and SL Atkin. Somatostatin receptors 2 and 5 are preferentially expressed in proliferating endothelium. *British Journal of Cancer* 92: 1493-1498, 2005.

62. Matin, SF, PT Tinkey, AT Borne, LC Stephens, A Sherz, and DA Swanson. A pilot trial of vascular targeted photodynamic therapy for renal tissue. *Journal of Urology* 2008 May 20. [Epub ahead of print].

63. Chen, B., BW Pogue, PJ Hoopes, and T Hasan. Vascular and cellular targeting for photodynamic therapy. *Critical Reviews in Eukaryotic Gene Expression* 15(4): 279-305, 2006.

64. Peng, Qian, Trond Warloe, Kristian Berg, Johan Moan, Magne Kongshaug, Karl-Erik Giercksky, and John M. Nesland. *Cancer* 79(12): 2282-2308, 1997.

65. Hensler, Thorsten, Heike Hecker, Klaus Heeg, Claus-Dieter Heidecke, Holger Bartels, Winfried Barthlen, Hermann Wagner, Jorg-Rudiger Siewert, and Bernhard Holzmann. Distinct mechanisms of immunosuppression as a consequence of major surgery. *Infection and Immunity* 65(6): 2282-2291, 1997.

66. Amos CI, Wu X, Broderick P, Gorlov IP, J Gu J, T Eisen T, Dong Q, Zhang Q, Gu X, Vijayakrishnan J, Sullivan K, Matakidou A, Wang Y, Mills G, Doheny K, Tsai YY, Chen WV, Shete S, Spitz MR, Houlston RS. Genome-wide association scan of tag SNPs identifies susceptibility locus for lung cancer at 15q25.1. *Nature Genetics.* 40(5): 616-622, 2008.